Abstract

Fesselin and caldesmon: natively unfolded proteins in smooth muscle regulation

by

Svetlana Hamden

May 2010

Committee chair: Joseph M. Chalovich

Department: Biochemistry and Molecular Biology

Dysregulation of smooth muscle contraction is linked to diseases such as atherosclerosis, asthma, hypertension, urinary incontinence, premature birth and others. The goal of this project is to contribute to our understanding of the mechanisms of smooth muscle regulation. Caldesmon and fesselin are actin-binding proteins abundant in smooth muscle that have multiple binding partners and are well positioned to alter smooth muscle contraction. Because fesselin is a heat-stable proline rich protein that has many properties in common with the natively unfolded COOH terminal fragment of caldesmon, we sought to determine whether fesselin is natively unfolded. We compared fesselin to a known globular protein (myosin S1) and the unfolded C-terminal 22 kDa fragment of caldesmon (CaD22) using techniques such as gel filtration, intrinsic tryptophan

fluorescence and circular dichroism. We showed that fesselin is a natively unfolded protein. We also investigated the effects of phosphorylation by p^{21}-activated kinase 3, PAK, and calmodulin on CaD22. We found a novel regulatory region between the residues 627-642 in the unfolded caldesmon C-terminus and identified four minor residues slowly phosphorylated by PAK. Phosphorylation of this region alters both the ability of caldesmon to inhibit actomyosin ATPase and the interactions between caldesmon and Ca^{2+}-calmodulin that may contribute to the overall regulation of caldesmon's activity.

Fesselin and caldesmon: natively unfolded proteins in smooth muscle regulation

A Dissertation

Presented To

The Faculty of the Department of Biochemistry and Molecular Biology

East Carolina University

In Partial Fulfillment

of the Requirements for the Degree

Doctor of Philosophy

by

Svetlana Hamden

May 2010

Fesselin and caldesmon: natively unfolded proteins in smooth muscle regulation

by

Svetlana S. Hamden

APPROVED BY:

DIRECTOR OF DISSERTATION: _____

Dr. Joseph Chalovich

COMMITTEE MEMBER: _____

Dr. Brian Shewchuk

COMMITTEE MEMBER: _____

Dr. David Cistola

COMMITTEE MEMBER: _____

Dr. Colin Burns

ACTIN DEAN OF THE GRADUATE SCHOOL: _____

Dr. Paul Gemperline

ACKNOWLEDGEMENTS

I am thankful to my mentor, Dr. Joseph Chalovich, who continually conveyed a spirit of adventure and excitement in regard to research and gave his encouragement, supervision and support. I would like to thank Dr. Kenney, Dr. Hoffman, Dr. Burns, Dr. Schroeter and my labmates who helped me with my experiments. And also my son Andis and my husband Khalief, the most important people in my life, for their love and understanding during the course of this work.

TABLE OF CONTENTS

CHAPTER I. INTRODUCTION

Smooth muscle is an involuntary non-striated muscle, found within many vital organs, such as arteries and veins, bladder, uterus, male and female reproductive tracts, gastrointestinal tract, respiratory tract, the ciliary muscle, and iris of the eye. Malfunction of smooth muscle contraction has been implicated to play a role in a large number of diseases, such as atherosclerosis, hypertension, asthma, irritable bowel syndrome, urinary incontinence and premature birth. Nonmuscle cells share similarities with smooth muscle cells in terms of regulation of contraction. Nonmuscle cells are important in other disorders such as cancer. Better understanding of mechanisms of regulation of smooth muscle contraction may lead to therapies for the aforementioned disorders.

My goal in this thesis is to investigate means of altering smooth muscle contraction by focusing on regulatory proteins that are abundant in smooth muscle. Caldesmon and fesselin are natively unfolded actin binding proteins that have multiple binding partners (Permyakov et al 2003, Khaymina et al 2007). The biological function of these proteins is not totally clear but it is clear that these proteins are excellent targets.

Mechanisms of smooth muscle contraction

Like any muscle, smooth muscle is made up primarily of two kinds of filaments: the thick myosin filaments and the thin actin filaments that contain actin and other regulatory proteins (Figure 1A). Muscle contraction is caused by the sliding of myosin and actin filaments over each other. The sliding of the filaments happens when the globular heads protruding from myosin filaments attach and interact cyclically with actin filaments to form

cross-bridges, moving along actin by a kind of rowing action. The energy for this is provided by the hydrolysis of ATP that produces a conformational change in myosin and causes movement.

Regulation of smooth muscle contraction

Smooth muscle contraction is regulated by changes in both myosin and actin filaments.

Myosin-linked regulation

Myosin-linked regulation is better characterized and involves calcium-regulated phosphorylation of myosin. The myosin heads are made up of heavy chains and light protein chains. In order for cross-bridge cycling to occur, myosin light chain kinase (MLCK) must phosphorylate the 20-kDa light chain of myosin (Gao et al. 2001), causing myosin to switch from a "folded" conformation with very low ATPase activity (10S form) to an "extended" active conformation (6S form) and turning on the myosin ATPase, as shown in Figure 1B (Sellers and Knight, 2007). When the muscle is stimulated to contract, the intracellular concentration of calcium ions is increased. Calcium binds to calmodulin, and the calcium-calmodulin complex activates MLCK allowing myosin to become phosphorylated and activated.

MLCK is the target for phosphorylation by cyclic AMP-dependent protein kinase (Conti and Adelstein, 1981), protein kinase C (Ikebe et al. 1985, Nishikawa et al. 1985) and calmodulin-dependent protein kinase II (Hashimoto and Soderling, 1990). Phosphorylation by any of these kinases reduces the affinity of MLCK for calcium-calmodulin thus preventing activation of MLCK by calcium-calmodulin.

The state of myosin light chain phosphorylation is further regulated by MLC phosphatase, which dephosphorylates the myosin light chains and inhibits the contraction (Figure 2). (Adelstein and Sellers, 1987).

Myosin may also be regulated by binding to specific ligands. Ligands could function by changing the size of myosin filaments or by changing the conformational state of myosin. For example, smooth muscle myosin filaments are much less stable than skeletal muscle filaments. ATP easily disassembles the dephosphorylated smooth muscle myosin filaments into monomers (but not phosphorylated ones). Caldesmon stabilizes smooth myosin thick filaments and cross-links them with actin filaments (Katayama et al. 1995).

Telokin binding to myosin suppresses its folding into the 10S conformation keeping myosin in its active 6S state (Masato et al. 1997). This seems to be a common mechanism for regulating motor proteins. Kinesin-1 is able to fold in a regulatory manner similar to myosin (Hackney et al. 1992; Stock et al. 1999). Proteins JIP-1 and FEZ1, upon binding to kinesin-1, are able to activate it (Blasius et al. 2007). Similarly, myosin-binding proteins might regulate myosin by altering the equilibrium between 10S and 6S forms of myosin.

The exact role of caldesmon and fesselin in the regulation of smooth muscle contraction is not completely clear yet.

Figure 1. A. Scematic diagram showing the structure of the sarcomere. B. Schematic representation of inactive (10S) and active (6S) myosin forms and myosin filaments. C. Schematic representation of G-actin, F-actin and acto-myosin interaction.

A.

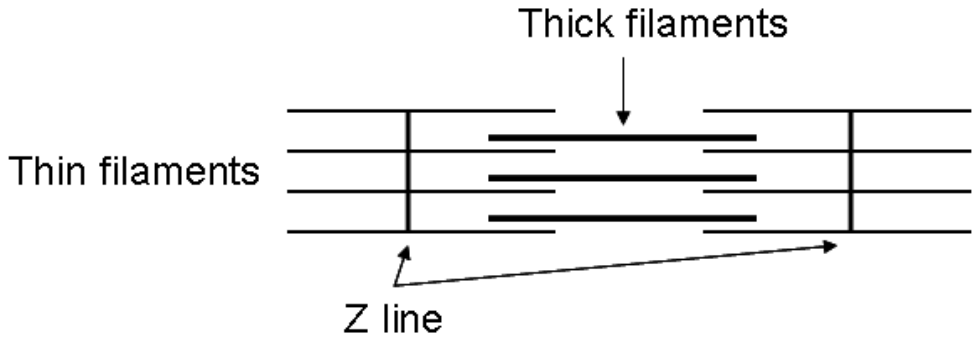
Thick filaments
Thin filaments
Z line

B.

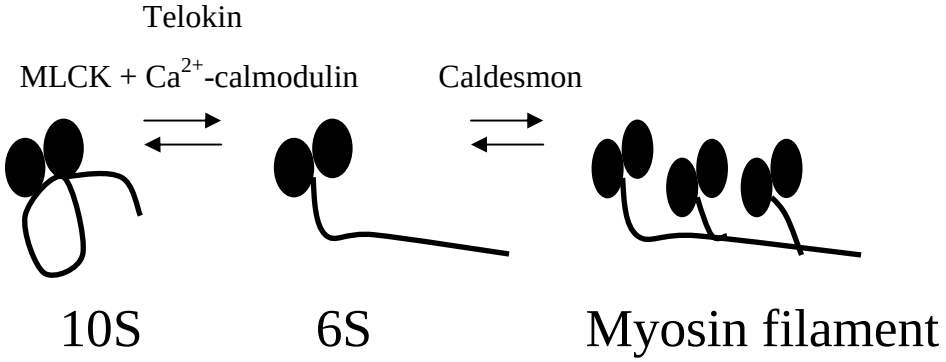
Telokin
MLCK + Ca2+-calmodulin
Caldesmon
10S
6S
Myosin filament

C.

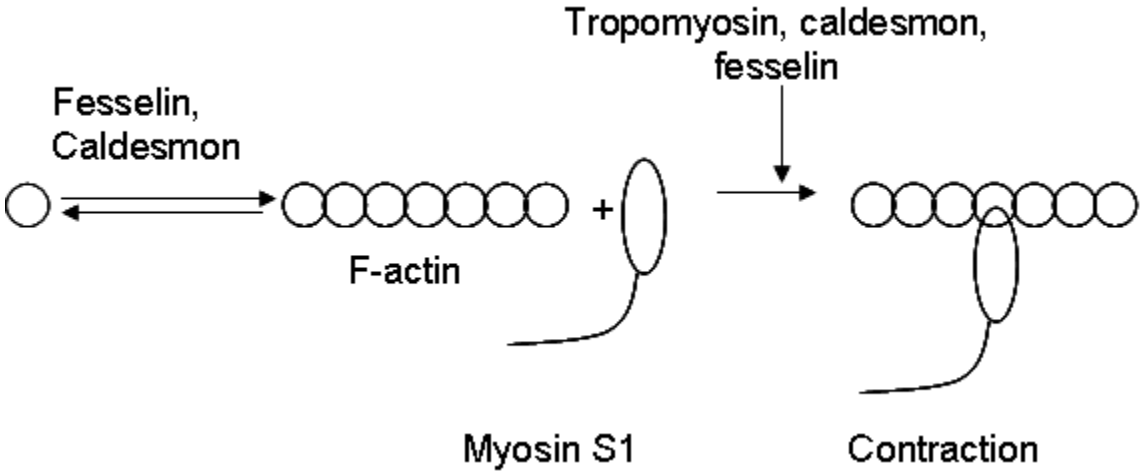
Tropomyosin, caldesmon, fesselin
Fesselin, Caldesmon
F-actin
Myosin S1
Contraction

Figure 2. Schematic representation of myosin-linked regulation of smooth muscle contraction.

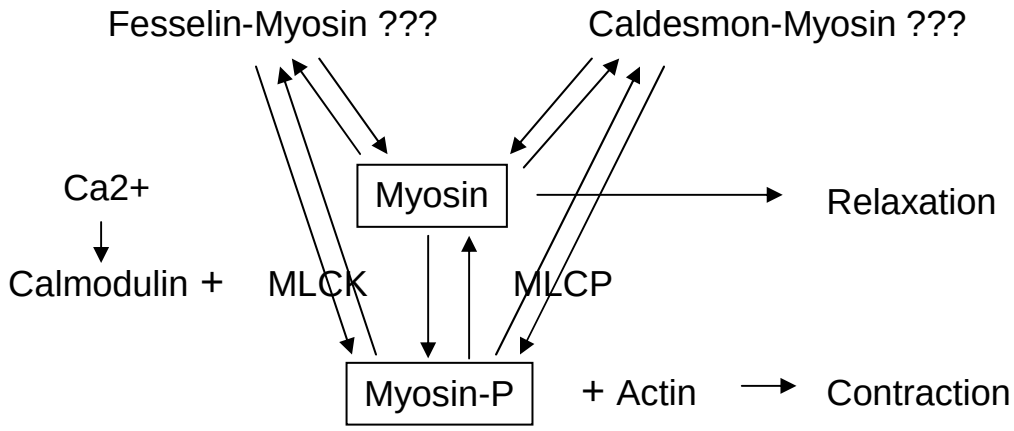
Fesselin-Myosin ???
Caldesmon-Myosin ???
Ca2+
Myosin
Relaxation
Calmodulin +
MLCK
MLCP
Myosin-P
+ Actin
Contraction

Actin-linked regulation

While myosin phosphorylation is generally thought to be essential for smooth muscle contraction to occur, actin-binding proteins may modulate contractility by both indirect and direct mechanisms.

An example of an indirect mechanism is modulation of actin polymerization/depolymerization. Actin alone polymerizes slowly because of the rate-limiting process of nucleation. Proteins such as caldesmon (Galazkiewicz et al. 1989), fesselin (Beall and Chalovich, 2001), Arp2/3 (Pollard et al. 2000) and other accelerate actin assembly from monomeric G-actin form into F-actin (Figure 1C). Caldesmon, tropomyosin and other proteins protect actin filaments from severing and disassembly (Dabrowska et al. 1996).

Actin-binding proteins may also directly control the force producing interaction between actin and myosin. Caldesmon, tropomyosin and possibly fesselin can alter actin-myosin interactions and regulate contraction. Tropomyosin can occupy different positions on the actin surface that may or may not obstruct myosin-binding sites on actin (Xu et al. 1999). The presence of tropomyosin on actin filaments introduces cooperativity to the interaction between actin and myosin because tropomyosin interacts with seven actin subunits (Greene and Eisenberg 1980). Caldesmon and fesselin are also interesting because both of them bind to actin (Sobue et al. 1981; Leinweber et al 1999), myosin (Hemric and Chalovich, 1988; Schroeter and Chalovich 2005) and calmodulin (Sobue et al. 1981; Schroeter and Chalovich, 2004) and inhibit actomyosin ATPase activity (Ngai and Walsh, 1984; Schroeter and Chalovich 2005).

Both proteins seem to participate in many if not all of the levels of regulation of smooth muscle contraction.

Actin-binding proteins also maintain the unique organization of the contractile apparatus in smooth muscle. Unlike skeletal muscle, in smooth muscle no striation is seen under the microscope, giving a “smooth” appearance. Instead, the actin filaments are organized through attachment to dense bodies (Heumann, 1970; Uehara et al. 1971) that are the equivalent of Z-disks in striated muscle. In smooth muscle, thick and thin filaments together with dense bodies form contractile units that are connected to each other by intermediate filaments. Figure 3 is a schematic illustration demonstrating the suggested arrangements of contractile elements in smooth muscle. Actin filaments are linked to the plasma membrane at the dense plaques and within the cell to cytoplasmic dense bodies that contain such proteins as alpha-actinin (Lazarides 1976; Fay et al. 1983) and fesselin (Renegar et al. 2009).

Figure 3. The suggested arrangements of contractile and cytoskeletal elements in smooth muscle. Actin and myosin filaments are depicted as long, thin lines or short, thick lines, respectively. Wavy lines represent intermediate filaments. Dense plaques and dense bodies correspond to the closed triangles and the closed circles, respectively.

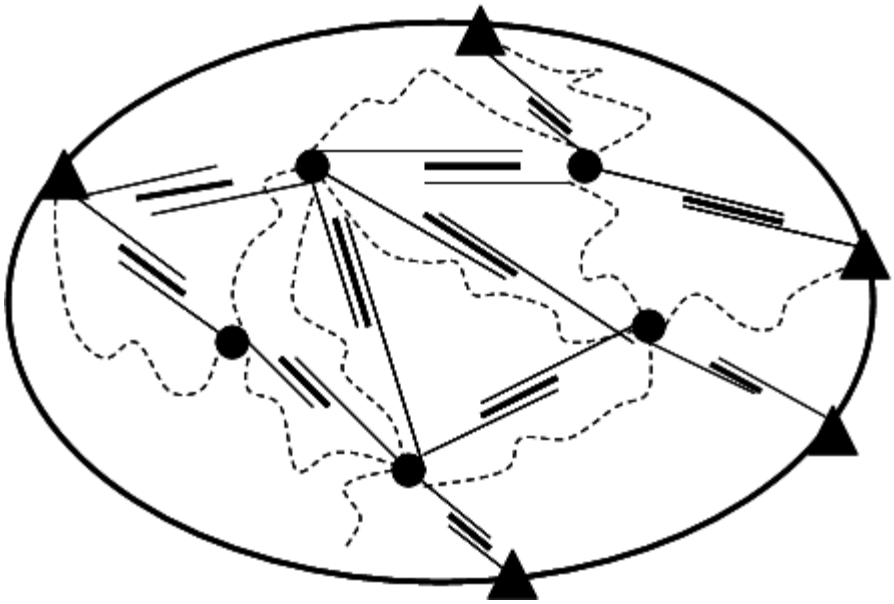

Caldesmon

Caldesmon is found in smooth muscle cells and also in non-muscle cells. It is of great importance as in smooth muscle it substitutes for troponin, one of the main regulators of skeletal muscle contraction (Kamm and Stull 1985). Perhaps the best evidence of an *in vivo* role of caldesmon is increase in caldesmon protein content during pregnancy that contributes to the suppression of contractility of pregnant myometrium. During labor the inhibition is reversed to achieve uterine contractions (Li et al. 2003). That serves as strong evidence that caldesmon plays a crucial role in regulation of muscle contraction and motility. But the full range of caldesmon functions still remains unknown.

Structure of caldesmon

Caldesmon has an elongated shape and can be roughly divided into three parts (Figure 4). The N-terminal part houses myosin-binding sites and interacts weakly with Ca^{2+}-Calmodulin and actin. The middle part, also known as the “spacer”, contains a highly charged alpha-helical repeating sequence (Bryan 1989) and has no clear binding properties. The spacer is present only in h-caldesmon (high molecular mass caldesmon) which is a smooth muscle form of caldesmon. The middle part is deleted in non-muscle isoform of caldesmon, or l-caldesmon (low molecular mass caldesmon) (Bryan and Lee 1991). The C-terminal part contains almost all of the functional properties of the molecule, such as actin, tropomyosin and Ca^{2+}-Calmodulin binding (Szpacenko and Dabrowska, 1986; Wang et al. 1991), inhibition of the actomyosin ATPase activity (Fujii et al 1987) and many phosphorylation sites. The C-terminal region of caldesmon is also intrinsically unstructured (Permyakov et al 2003). The importance of the unfolded structure of this region is discussed below.

Figure 4. Domain structure of smooth-muscle caldesmon. The nomenclature corresponds to chicken h-caldesmon.

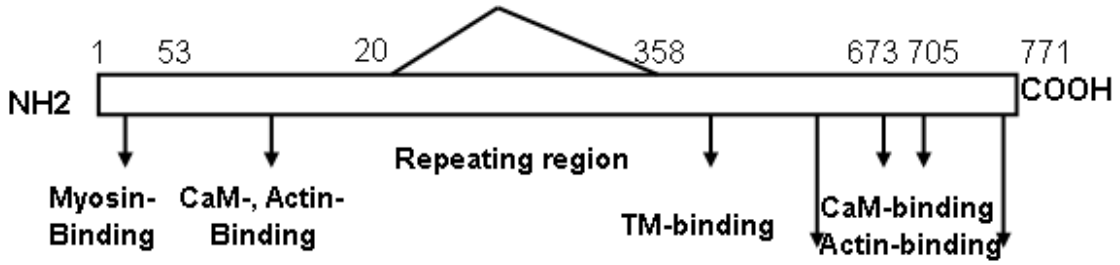
1
53
20
358
673 705
771
NH2
COOH
Repeating region
Myosin-
Binding
CaM-, Actin-
Binding
TM-binding
CaM-binding
Actin-binding

Regulation by caldesmon

Caldesmon has many functions in the cell. It can polymerize actin (Galazkiewicz et al. 1989), bundle actin filaments (Bretcher 2004), polymerize myosin filaments (Katayama et al. 1995), and inhibit actin-activated myosin ATPase (Ngai and Walsh, 1984). For caldesmon to regulate actin polymerization and actin activation of myosin ATPase activity it is necessary that the effects of caldesmon be variable. Both calcium-calmodulin binding and caldesmon phosphorylation are known to influence the affinity of caldesmon to its various binding partners and also change the activity of caldesmon even when bound to its partners.

Regulation of actin polymerization by caldesmon.

Caldesmon has a capacity to polymerize G-actin, by stimulating the nucleation phase (Galazkiewicz et al. 1989). When bound to Ca^{2+}-calmodulin, caldesmon is unable to initiate polymerization of actin (Galazkiewicz et al. 1985). Phosphorylation of caldesmon by MAPK (Huang et al. 2003) and cdc2 kinase (Yamashiro et al. 1990) reduces its binding to actin and hence might also negatively affect the ability of caldesmon to initiate actin polymerization. It is unclear how important this function of caldesmon is *in vivo*, since many proteins such as Arp2/3 are much more potent actin polymerizers (Goley and Welch, 2006). Arp2/3 complex has been shown to trigger podosome formation in dynamic cells (Yamaguchi et al. 2005). Caldesmon competes with Arp2/3 for actin binding and inhibits podosome formation thus regulating the ability of the cell to invade tissues (Morita et al. 2006).

Regulation of myosin by caldesmon.

Caldesmon binding to myosin has been shown to induce the formation of myosin filaments under the conditions where myosin alone is disassembled, and tether myosin filaments to actin filaments (Katayama et al 1995). Calcium-calmodulin reduces the binding of caldesmon to myosin (Ikebe and Reardon, 1988). Phosphorylation of caldesmon by calmodulin-dependent kinase II also weakens the binding of caldesmon to myosin (Sutherland and Walsh, 1989).

Regulation of actin-activated myosin ATPase by caldesmon.

Numerous studies have demonstrated that caldesmon acts as an inhibitor of the actomyosin ATPase, although there is an ongoing debate in the field on what the mechanism of the inhibition is (Chalovich et al. 1998; Chalovich et al. 1990; Marston and Redwood, 1992; Alahyan et al 2006). In the presence of calcium, calmodulin reverses the inhibititory activity of caldesmon toward actin stimulated ATPase activity. This is a complex effect that involves a weakening of its binding to actin and actin-tropomyosin (Hodgkinson et al 1997). Some reports show that the ability of caldesmon to inhibit ATPase activity is attenuated even when caldesmon remains bound to actin (Pritchard and Marston, 1989).

Phosphorylation of caldesmon by kinases such as MAPK (Redwood et al. 1993), cdc2 (Yamakita et al. 1992), PAK (Foster et al. 2000), PKC (Vorotnikov et al 1994), Ca^{2+}-calmodulin kinase II (Ngai and Walsh, 1987) also releases the inhibition of the ATPase activity. The phosphorylation residues for these kinases have been determined (Figure 5).

Effect of Ca^{2+}-calmodulin binding and phosphorylation on the conformation of caldesmon.

The C-terminal region of caldesmon is natively unfolded (Permyakov et al. 2003), and its conformation can be easily modified by a ligand binding and/or phosphorylation.

Calmodulin binding was shown to have a distinct structural effect on the unfolded C-terminal region of caldesmon. Binding to calmodulin is capable of inducing alpha-helix formation in the synthetic caldesmon fragments (Zhou et al. 1997). Huang et al (2003) observed that when caldesmon was bound to actin, both Ca^{2+}-calmodulin binding and phosphorylation by MAPK caused a moderate elongation in their caldesmon fragment, as detected by Fluorescence Resonance Energy Transfer method (FRET).

No structural data has been reported yet on the phosphorylation of caldesmon by PAK kinase.

Kinases that phosphorylate caldesmon *in vivo*

There has been an extensive discussion about which kinase is a key regulator of caldesmon *in vivo* and which phosphorylation sites are involved in regulation (Gorenne et al. 2004; Redwood et al. 1993; Childs et al. 1992). It is possible that several kinases are involved, but currently evidence exists for regulation of CaD by phosphorylation *in vivo* by MAP kinase (Adam et al. 1993; D'Angelo et al. 1999), PAK kinase (Eppinga et al. 2006) and cdc2 kinase (Yamashiro et al. 1991) whereas evidence to support the involvement of other kinases *in vivo* is still scarce.

Figure 5. Phosphorylation sites on CaD22. All phosphorylation sites are in bold. PAK kinase sites are in square brackets. MAPK sites[1], Calmodulin kinase II sites[2], cdc2 kinase sites[3] and PKC sites[4] are indicated with superscripts as shown. The tropomyosin-binding region has a single underline. The calmodulin-binding regions have a double underline. The residue numbers at the beginning and at the end of the sequence are in curly brackets.

{563}MKEEIERRRAEAAEKRQKVPEDGVSEEKKPFKCFS[3]PKGS**S**[2,4]LKIEERAEFLNK

SAQKSGMKPAHTTAVVSKID**S**[2]RLEQYTSAVVGNKAAKPAKPAASDLPVPAEGVRN

IK[**S**]MWEKGNVFSS[3]PGGTGT[3]PNKETAGLKVGVS[**S**]RINEWLTKT[3]PEGNK**S**[1,3]PAP

KPSDLRPGDVSGKRNLWEKQ**S**[2,4]VEKPAASSSKVTATGKKSETNGLRQFEKEP{771}

p21-activated kinase (PAK)

PAK kinase is emerging as a major regulator of Caldesmon. First, by using an antibody specific to PAK phosphorylation sites on caldesmon PAK was shown to phosphorylate caldesmon *in vivo* (Eppinga et al. 2006). Second, constitutively active PAK3 produces Ca^{2+}- independent contraction of smooth muscle that coincides with an increase in caldesmon phosphorylation (Van Eyk et al. 1998). Third, PAK kinase appears to be an important regulator of caldesmon-mediated actin dynamics (Eppinga et al. 2006; Dharmawardhane et al, 1997) and cell motility (Jiang et al. 2010) *in vivo*.

PAK is a serine/threonine protein kinase and a downstream effector of Rac and Cdc42 GTPases. Foster et al. 2000 found that PAK phosphorylated caldesmon to a maximum of 2 mol phosphate per mol caldesmon within 120 minutes, but the longer incubation times have not been investigated. The phosphorylation sites for PAK were identified as Ser672 and Ser702 of chicken gizzard caldesmon. These sites are adjacent to the calmodulin-binding sites, and were less accessible to PAK when caldesmon was bound to calmodulin. PAK phosphorylation weakened Ca^{2+}-calmodulin binding to caldesmon by approximately 10-fold. Caldesmon phosphorylated by PAK did not significantly change its affinity for actin-tropomyosin, only a modest reduction in affinity was reported with K_d increase less that 2-fold. However it was significantly less effective in inhibiting actomyosin ATPase activity. PAK-phosphorylated caldesmon inhibited actin-activated myosin S1 ATPase by about 40%, whereas unphosphorylated caldesmon was able to inhibit actin-activated myosin S1 ATPase to about 80% (Foster et al. 2000).

Both phosphorylation and calmodulin binding may occur in smooth muscle cells and non muscle cells. An important question is how these two signaling mechanisms work together to alter the effects of caldesmon.

Fesselin

Fesselin is a protein that was discovered in Dr. Chalovich's lab in 1999 by Dr. Barbara Leinweber (Leinweber et al. 1999). It is a member of the synaptopodin family of proteins (Schroeter et al. 2008). Other members of this family include synaptopodin and myopodin, both of which are proline-rich actin-associated proteins. Fesselin shares 96% identity with synaptopodin 2 also known as myopodin, and is only 47.4% homologous to synaptopodin, with the highest degree of homology residing in the C-terminal half on the molecules.

Synaptopodin

Synaptopodin is expressed in differentiated kidney glomerular podocytes and telencephalic dendrites (Mundel et al. 1997). The expression is restricted to later stages of cellular differentiation. It can directly bind to actin and bundle actin filaments. Synaptopodin plays a role in modulating the actin-based shape and motility of dendritic spines and podocyte foot processes. Synaptopodin-deficient mice lack the dendritic spine apparatus and display impaired activity-dependent long-term synaptic plasticity (Deller et al. 2003).

Myopodin

Myopodin is found at the Z-disks of myoblasts (Weins et al. 2001). Myopodin is also able to translocate into the nucleus under stress conditions. Myopodin was proposed to play a dual role as a structural protein at the Z-disk and as a regulator protein participating in a signaling

pathway between the nucleus and the Z-disk during development and in situations of cellular stress. It was shown that frequent complete or partial deletions of the myopodin gene occurred among bladder (Sanchez-Carbayo et al. 2003) and prostate (Jing et al. 2004) cancer cases. But the exact functions of these proteins are still unknown.

Properties of fesselin

Unlike other members of the synaptopodin family of proteins, fesselin can be readily isolated from heat treated extracts of avian gizzard muscle (Leinweber et al. 1999). Fesselin binds to a variety of proteins, such as myosin (Schroeter and Chalovich, 2005), actin (Leinweber et al. 1999), alpha-actinin (Pham and Chalovich, 2006) and calmodulin (Schroeter and Chalovich, 2004). Fesselin bundles actin filaments (Leinweber et al, 1999). This property of fesselin is very important because it is known that actin filaments are usually disrupted in malignant cells (Rao and Li, 2004). Fesselin and other actin bundling proteins might provide the basis for maintaining cell morphology and preventing metastases. Fesselin also induces actin polymerization (Beall and Chalovich, 2001) and this activity is regulated by Ca^{2+}-calmodulin (Schroeter and Chalovich, 2004). Myosin S1 competes with fesselin for binding to actin or to actin-tropomyosin and fesselin inhibits actin activation of S1 ATPase activity (Schroeter and Chalovich, 2005). It was observed that fesselin is associated with dense bodies in smooth muscle tissue (Renegar et al. 2009). Hence, it is likely that fesselin is involved in the regulation of smooth muscle contraction.

Similarities between caldesmon and fesselin

Fesselin shares many features with caldesmon. Both fesselin and caldesmon are actin-binding proteins, their binding affinity is moderate (Velaz et al. 1989; Leinweber et al. 1999). They stimulate actin polymerization (Galazkiewicz et al. 1985; Beall and Chalovich, 2001) and actin bundle formation (Bretscher, 1984; Leinweber et al. 1999). Both proteins compete with S1 myosin for actin binding and can bind to myosin themselves, although the binding occurs in the different regions of myosin (Hemric and Chalovich, 1988; Schroeter and Chalovich, 2005). Fesselin and caldesmon also bind to Ca^{2+}-calmodulin (Schroeter and Chalovich, 2004; Sobue et al. 1981). Both proteins inhibit actomyosin ATPase activity (Ngai and Walsh, 1984; Schroeter and Chalovich, 2005). However, inhibition by caldesmon can be reversed by Ca^{2+}-calmodulin (Szpacenko et al. 1985) and phosphorylation (Ngai and Walsh, 1984). Inhibition by fesselin is not regulated by Ca^{2+}-calmodulin or any other regulatory mechanisms thus far identified. It is not clear whether fesselin regulates contraction directly.

Another feature that both proteins share is that both are able to refold rapidly since both can be prepared after a heat treatment step. This and all of the above features make sense for caldesmon since it is a natively unfolded protein. The similarity of caldesmon and fesselin made us wonder whether fesselin was a natively unfolded protein too.

Natively Unfolded proteins

Natively Unfolded (or often referred to as intrinsically unstructured or disordered) proteins are characterized by lack of stable tertiary structure under physiological conditions (Wright and Dyson, 1999; Dunker et al.

2002). It is now known that a large number of proteins encoded by the genome contain little or no ordered secondary or tertiary structure under physiological conditions. Interestingly, intrinsic disorder is more prevalent in complex organisms. Eukaryotes contain 35-51% long unstructured regions whereas bacteria and archaea contain 7-33% and 9-37%, respectively, as calculated by disorder prediction tool PONDR VL-XT (Dunker et al. 2000). The evolutionary persistence of such proteins represents strong evidence in the favor of their importance.

Intrinsically unstructured proteins are of great interest as they appear to go against the biochemistry dogma that the folded 3D-structure is absolutely essential for biological activity. Their structures resemble the denatured states of ordered proteins, and they exist as an ensemble of rapidly interconverting structures (Sickmeier et al. 2007).

The hallmarks of natively unfolded proteins are larger hydrated volumes, little or no secondary structure, increased intramolecular flexibility, and unusual responses to environmental changes such as having increased structure at high temperatures or at extreme pH values (Uversky, 2002a). Natively unfolded proteins may be either coil-like (completely unstructured) or premolten globule-like (containing a bit of localized structure) (Uversky, 2002b).

The act of binding often causes regions of natively unfolded proteins to adopt different structures upon binding to different targets. The extent of structural changes upon binding ranges from no change, when a protein continues to constantly fluctuate between a large number of conformational states, to a drastic conformational switch or loss of structure (Tompa et al. 2005).

Special very flexible short elements have been proposed to mediate binding (Preformed Structural Elements, PSEs, or Molecular Recognition Features, MoRFs). These elements consist of short regions of intrinsic disorder that have strong intrinsic preference for the conformation they adopt when bound to their partners (Oldfield et al. 2005).

The functions of natively unfolded proteins are vast. Unfolded regions often form flexible linkers/spacers between domains that regulate the distance between the domains and allow them to move freely relative to each other in search for binding partners. Unstructured proteins have relatively low affinity for their binding partners (Dunker et al. 2002). It allows them to quickly detach from another protein, so that a cell can react quickly when necessary. Hence, they can be activators in key cellular processes, such as cell division or gene transcription. Disordered regions are preferred sites of protein modifications (Fuxreiter et al. 2007), such as phosphorylation or acetylation which are known to act as switches activating signaling pathways or targeting proteins for degradation. Unfolded regions allow binding to an array of different partners (Uversky, 2002b), leading to multitasking of the same protein. Consequently, natively unfolded proteins often act as “hubs”, or flexible scaffolds, for protein complexes (Dunker et al. 2005). Unfortunately, natively unfolded proteins are often involved in diseases, from cancer to folding diseases, such as Alzheimer’s and Parkinson’s (Xie et al. 2007).

Why many actin-binding proteins are natively unfolded?

Many actin-binding proteins have unstructured regions that may be important in regulation. Unfolded regions of troponin I have been proposed to be involved in actin binding and inhibition of muscle contraction

(Blumenschein et al. 2006). CaD22 is largely natively unfolded (Permyakov et al. 2003). Other examples include thymosin β4, WASP, dematin, addictin, etc. The unfolded regions are readily accessible to other proteins and provide an easy way to regulate binding to actin by post-translational modifications such as phosphorylation and by ligand binding.

It is known that Ca^{2+}-calmodulin binding to a COOH-terminal caldesmon fragment induces folding (Permyakov et al. 2003). Another disorder-to-order transition example involves structuring of unfolded region of troponin I upon interaction with actin (Blumenschein et al. 2006). It is possible that multiple signals, like phosphorylation and ligand binding (i.e. Ca^{2+}-calmodulin) may work synergistically by altering the structure of unfolded regions.

We wished to determine if phosphorylation of natively unfolded actin binding proteins causes functional effects and/or structural changes similar to those observed by ligand binding. One of the proteins we chose to look at is a natively unfolded caldesmon because in smooth muscle it substitutes for troponin, one of the main regulators of skeletal muscle contraction, hence it might be of great importance in regulation. Another protein is fesselin that shares many features with caldesmon, as reviewed above, and may be an anti-oncogene in the cell.

CHAPTER II. FESSELIN IS A NATIVELY UNFOLDED PROTEIN

Because fesselin shares many features with the natively unfolded C-terminal region of caldesmon we wanted to establish whether fesselin, like caldesmon, belongs to the family of natively unfolded proteins.

Results

Primary Structure Analysis.

We used several alrorithms to predict the fraction of disorder of fesselin from turkey meleagris gallopavo {GenBank: ABU55374.1}. The program PONDR (Combet et al. 2000) predicted the maximum amount of random coil (69.7%), while PreLink (Coeytaux et al. 2005), GlobPlot (Linding et al. 2003) and FoldUnfold (Galzitskaya et al. 2006) predicted 45-49% disorder.

All of the above algorithms predicted that fesselin contains unfolded regions interspersed with short structured regions (Fig. 6A). Further analysis of this sequence with PONDR predicted that the structure is 64-73% random coil, 16-25% alpha helix and 6-10% extended strand.

Natively unfolded proteins often have a greater net charge and a lower fraction of hydrophobic residues than folded proteins. Folded and unfolded proteins can often be distinguished by a charge-hydrophobicity plot (Uversky 2002a). Fig. 6B is a plot of the net charge versus the hydrophobicity for folded and natively unfolded proteins. The hydrophobicity and net charge of fesselin from turkey meleagris gallopavo were calculated using PONDR. Avian fesselin is at the border between unfolded and folded proteins. With these additional clues that fesselin could be natively unfolded, we examined physical properties of the protein fesselin that distinguish folded from unfolded proteins.

Analysis of the Stokes Radii of fesselin and Caldesmon22 by gel filtration chromatography and laser light scattering.

Unfolded proteins have larger stokes radii than folded proteins and therefore elute from gel filtration columns earlier than predicted from their masses. Figure 7A shows a plot of log (molecular weight) vs. elution time for a series of standard proteins. Myosin S1 falls on that standard curve as expected for a globular protein. However, both fesselin and Cad22 eluted earlier than expected for their molecular masses. We monitored molecular weight by light scattering to ensure that this was a real phenomenon. The molecular masses of fesselin and caldesmon obtained by light scattering were close to the expected masses, 73 kDa and 24 kDa, respectively. The apparent molecular masses of fesselin and Cad22 were 159 kDa and 115 kDa, respectively. These values correspond to Stokes radii of 5.3 nm and 4.6 nm, respectively. The expected Stokes radii were 4 nm for fesselin and 2 nm for Cad22. Fesselin has a Stokes radius that is 1.3x that expected for its molecular weight. Cad22 has a Stokes radius that is 2.4x its expected value. Therefore both fesselin and Cad22 have open structures.

Figure 7B shows plots of $\log(R_s)$ vs. log(M) for different conformational states of globular and natively unfolded proteins. Hydrodynamic data for fesselin were overlaid with these plots. Fesselin fell on the curve corresponding to premolten globule-like proteins. The data used to plot dependencies were taken from published results (Uversky 2002a; Tcherkasskaya et al. 2001).

FIGURE 6. A. Analysis using PONDR VLXT predictor. Fesselin is predicted to be largely unfolded, with several small structured regions. The location of the tryptophan residues within the sequence of fesselin is indicated by open circles. **B.** Charge-hydrophobicity plot for natively folded (black squares) and natively unfolded (white circles) proteins (Uversky 2002a). Superimposed are the data for fesselin (white hexagon). Fesselin falls on the border (solid line) between natively unfolded and natively folded proteins.

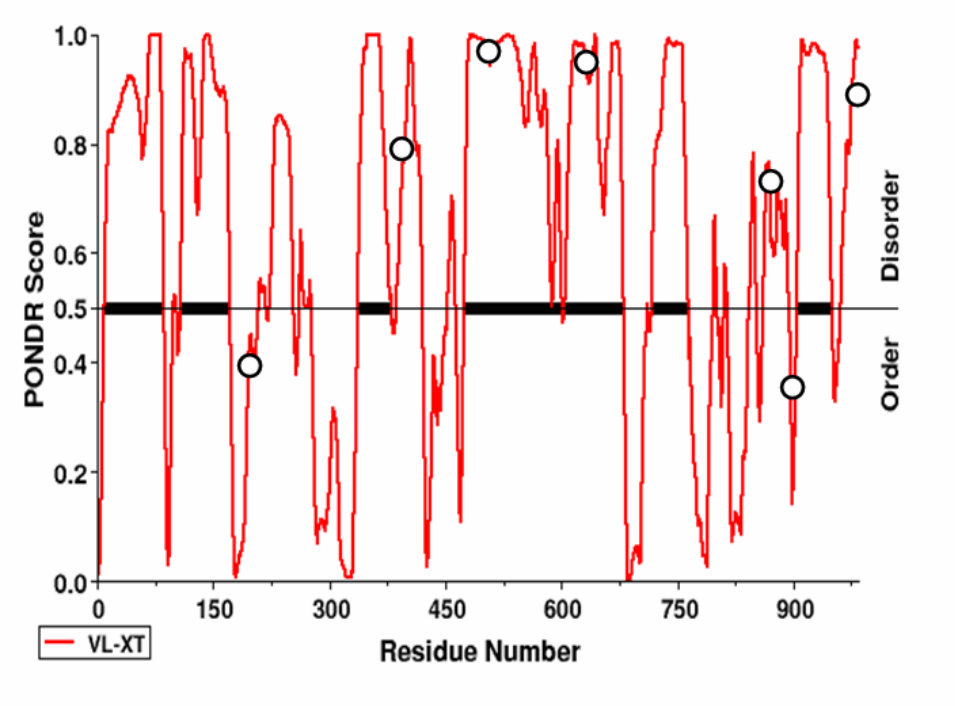
PONDR Score
1.0
0.8
0.6
0.5
0.4
0.2
0.0
Disorder
Order
0
150
300
450
600
750
900
Residue Number
VL-XT

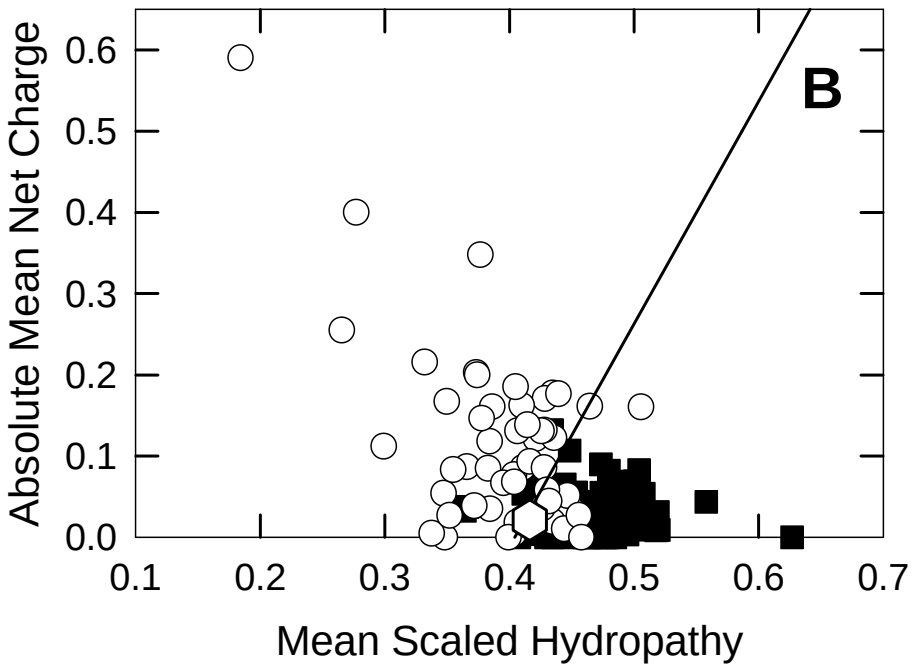
B
Absolute Mean Net Charge
0.6
0.5
0.4
0.3
0.2
0.1
0.0
0.1
0.2
0.3
0.4
0.5
0.6
0.7
Mean Scaled Hydropathy

FIGURE 7A. Both fesselin (solid circle) and Cad22 (solid square) are eluted earlier than expected for their molecular weights. The arrow indicates data for S1. **B.** Dependencies of Stokes radii (R_s) on molecular weight (M) for native globular proteins (squares), molten globules (circles), premolten globules (triangles), 6M guanidine HCl-unfolded proteins (diamonds), premolten globule-like state of natively unfolded proteins (filled triangles), and coil-like proteins (solid diamonds). Fesselin is shown as a white hexagon. The data used to plot the dependencies are taken from published results (Uversky 2002a; Tcherkasskaya et al. 2001).

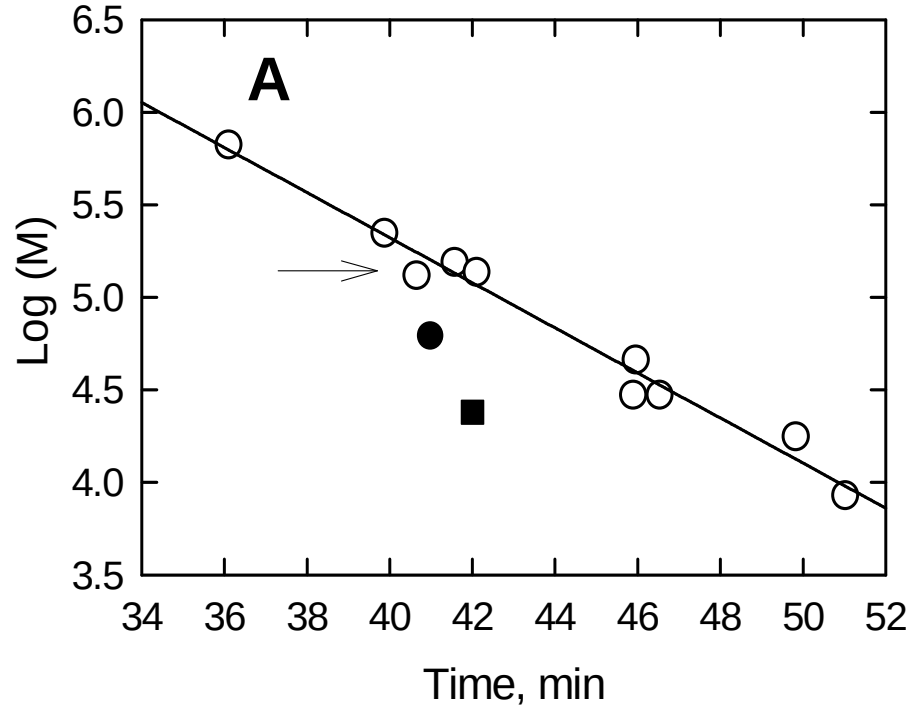
A
Log (M)
Time, min
6.5
6.0
5.5
5.0
4.5
4.0
3.5
34
36
38
40
42
44
46
48
50
52

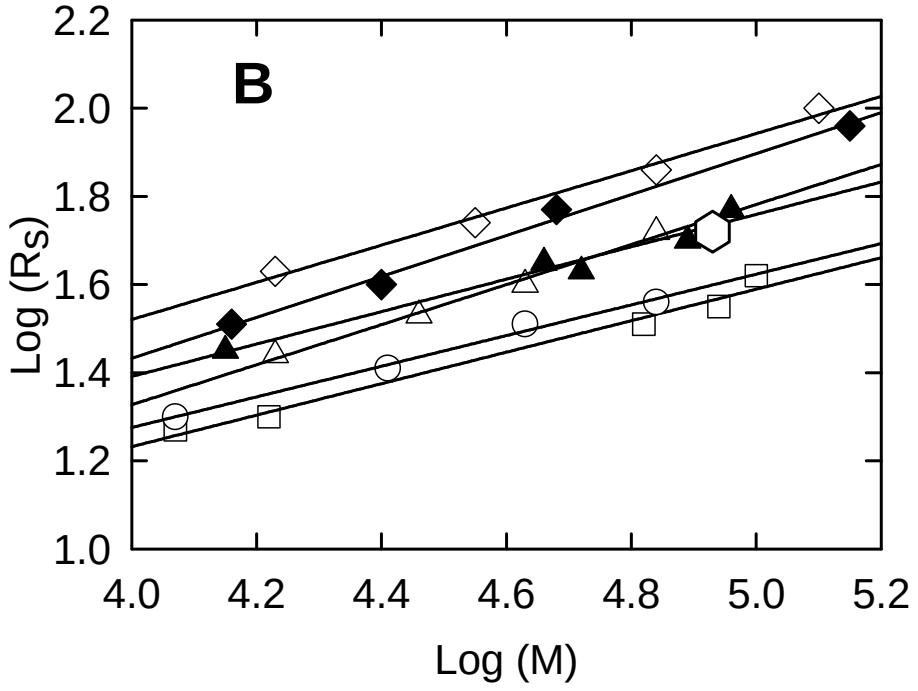
B
Log (Rs)
Log (M)
2.2
2.0
1.8
1.6
1.4
1.2
1.0
4.0
4.2
4.4
4.6
4.8
5.0
5.2

Analysis of intrinsic tryptophan fluorescence of S1, Cad22 and fesselin.

Another measure of the packing density of a protein is the exposure of its tryptophan residues to the solution. Tryptophan residues are normally buried in folded proteins. This burial shifts the fluorescence maximum from about 350 nm (typical for L-tryptophan in water solution) to about 335 nm as a result of shielding of tryptophan residues from the aqueous phase by the protein (Lakowicz 1983) Exposure of the tryptophan residues upon unfolding typically leads to an increase in quenching due to better accessibility of the fluorophores to quencher. The location of the tryptophan residues within the fesselin sequence is shown in Figure 6A.

Figure 8A shows that myosin S1 has a tryptophan fluorescence spectrum typical for a folded protein. The fluorescence maximum was centered at 334 nm, as expected in the case when tryptophan residues are buried inside the protein. Addition of sufficient guanidine hydrochloride to denature S1 led to a reduction in the intensity and a shift to a longer wavelength, 346 nm (Fig. 8A).

In contrast, both Cad22 (Fig. 8B), and fesselin (Fig. 8C) had spectra under native conditions that were typical of proteins with exposed tryptophan residues with maxima at 344 nm. Furthermore, the addition of 6M guanidine HCl had little effect on the spectra. The lack of effect of a denaturant confirms that the tryptophan residues were already exposed in both cases.

Exposure of the tryptophan residues was further investigated by the sensitivity of the spectra to a neutral quencher, acrylamide. Figure 9 shows the fluorescence intensity as a function of acrylamide concentration for S1, fesselin and Cad22. In the absence of a denaturant, S1 exhibited a linear

decrease in tryptophan fluorescence intensity with increasing acrylamide concentration. Upon addition of 6M guanidine HCl, the sensitivity to the quencher increased indicating increased exposure of tryptophan residues to the solvent. The non-linear relationship between the fluorescence and the quencher concentration could be due to the presence of both dynamic and static quenching.

The fluorescence intensities of tryptophan residues of both fesselin and Cad22 were more sensitive to the quencher in the absence of denaturant than was S1. This indicates a greater exposure of tryptophan residues of fesselin and Cad22 to the solvent. Furthermore, the curves obtained for fesselin and Cad22 were unchanged by the denaturant indicating that the structures are largely the same in the absence and presence of a denaturant. The upward curvature of the plot suggested dynamic and static quenching. The quenching constants were the same in the presence and absence of guanidine HCl suggesting that fesselin and Cad22 are unfolded under normal conditions (Fig. 9).

FIGURE 8. Effect of denaturatants on the tryptophan fluorescence for myosin S1 (A), Cad22 (B) and fesselin (C). Spectra were collected at 25^0C, either under native conditions (10 mM MOPS, 0.1 M KCl, 0.5 mM EDTA, 0.5 mM EGTA, pH 7.2) or in the same buffer containing 6 M guanidine HCl. Native spectra and spectra in the presence of 6 M guanidine HCl correspond to solid and dashed lines, respectively.

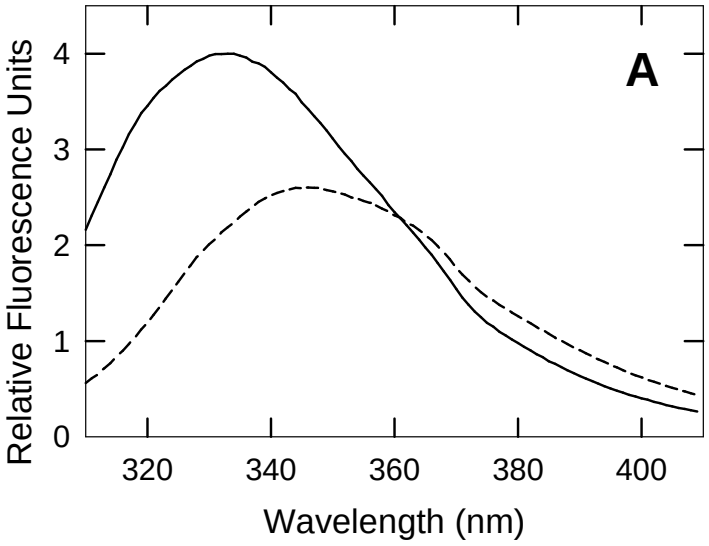
A
Relative Fluorescence Units
0
1
2
3
4
320
340
360
380
400
Wavelength (nm)

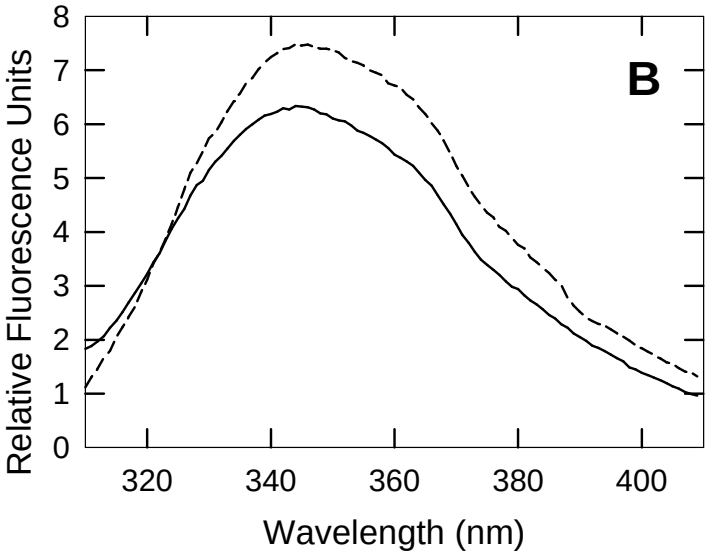
B
Relative Fluorescence Units
0
1
2
3
4
5
6
7
8
320
340
360
380
400
Wavelength (nm)

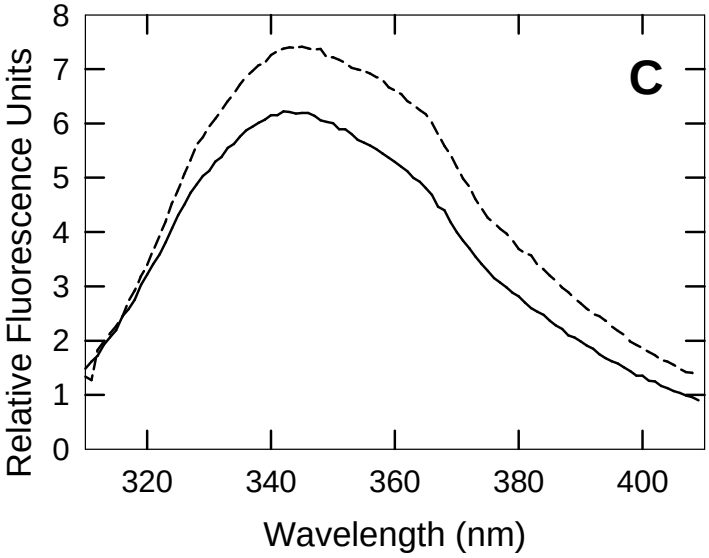
C
Relative Fluorescence Units
0
1
2
3
4
5
6
7
8
320
340
360
380
400
Wavelength (nm)

FIGURE 9. Stern-Volmer analyses of quenching of intrinsic tryptophan fluorescence of S1 (A), the 22 kDa caldesmon fragment (B) and fesselin (C). Data were collected at 25^{o}C either under native conditions,10 mM MOPS, 0.1 M KCl, 0.5mM EDTA, 0.5 mM EGTA, pH 7.2 (circles) or in the same buffer with 6 M guanidine HCl (squares). Solid lines correspond to the best fit of the equation 1: $F_0/F = 1 + (K_D + K_S)*[Q] + K_D*K_S*[Q]^2$, where F_0 and F are the fluorescence intensities in the absence and presence of quencher, respectively; K_D and K_S are the dynamic and static Stern-Volmer quenching constants, Q is the concentration of the quencher. The values of K_d and K_S determined for each experiment as follows: S1: Ks=0, Kd=4.43 M^{-1} (native conditions), Ks=1.54 M^{-1} and Kd=5.8 M^{-1} (guanidine HCl). CaD fragment: Ks=Kd=3.8 M^{-1} (native conditions), Ks=Kd=3.9 M^{-1} (guanidine HCl). Fesselin: Ks=Kd=4.6 M^{-1} (native conditions), Ks=Kd=4.4 M^{-1} (guanidine HCl).

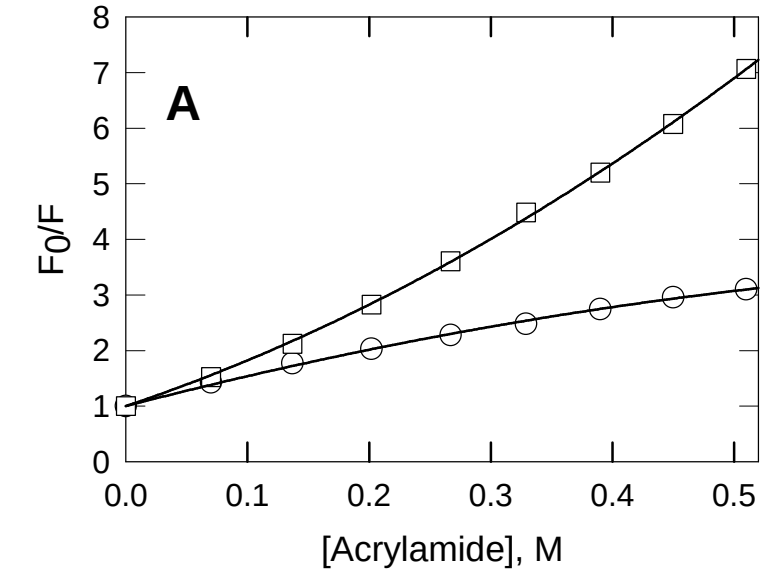
A
F0/F
[Acrylamide], M
0
1
2
3
4
5
6
7
8
0.0
0.1
0.2
0.3
0.4
0.5

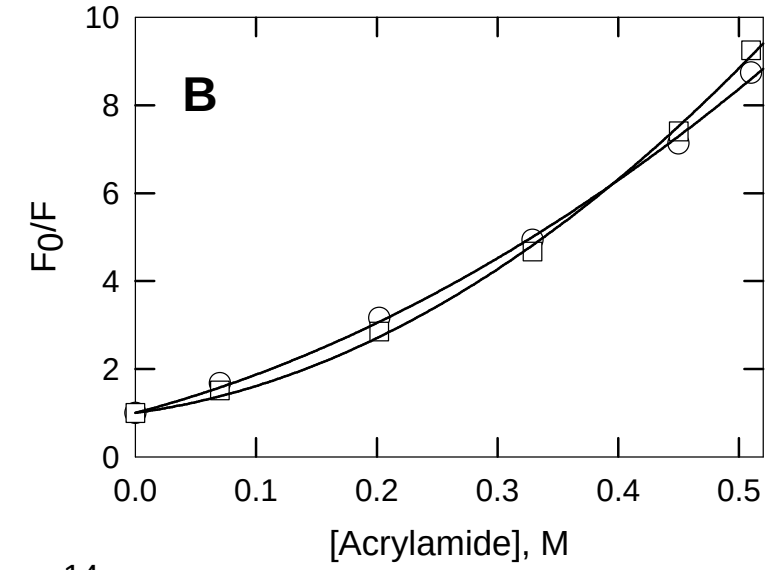
B
F0/F
[Acrylamide], M
0
2
4
6
8
10
0.0
0.1
0.2
0.3
0.4
0.5

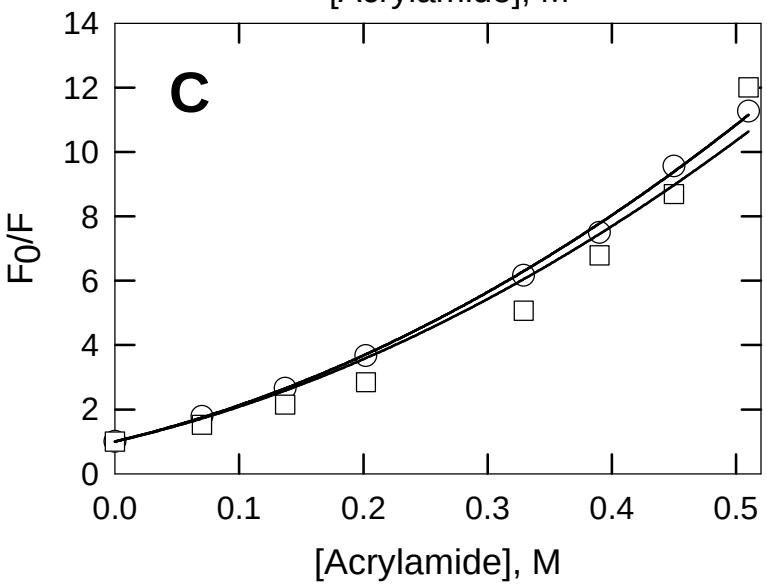
C
F0/F
[Acrylamide], M
0
2
4
6
8
10
12
14
0.0
0.1
0.2
0.3
0.4
0.5

Analysis of calmodulin binding to Cad22 and fesselin.

Both fesselin (Schroeter and Chalovich, 2005) and caldesmon (Sobue et al. 1981) bind to calmodulin. Calmodulin has already been shown to induce folding of Cad22 (Permyakov et al. 2003; Zhou et al. 1997) We examined the sensitivity of fesselin and Cad22 to acrylamide quenching in the presence of calmodulin to determine if calmodulin induces structure in fesselin as well. Calmodulin had a large effect on the quenching curve of Cad22 (Fig. 10A). The sensitivity of Cad22 to acrylamide was decreased when Cad22 was bound to calmodulin (squares). The quenching curve of fesselin was similarly affected by calmodulin binding but to a lesser degree. Figure 10B shows that the tryptophan residues of fesselin were protected by calmodulin.

The smaller effect seen with fesselin was likely the result of using intact fesselin rather than a calmodulin binding fragment of fesselin. We attempted to express a calmodulin binding domain of fesselin to further investigate possible induction of structure. That effort failed as described in Appendix 1.

FIGURE 10. Calmodulin binding to the 22 kDa caldesmon fragment (A) and to fesselin (B) protects the tryptophan residues from acrylamide quenching. Data are shown for the free protein (circles) and for the protein-calmodulin complex (squares). The conditions were 10 mM MOPS pH 7.2, 0.1 M KCl, 1 mM $CaCl_2$, at 25^{O}C. In all cases the curves exhibited complex quenching patterns that could be caused by both static and dynamic quenching. The following values of Kd and Ks were recovered from the best fit of Equation 1: Fesselin: Ks=Kd=4.5 M^{-1}; Fesselin-calmodulin: Ks=Kd=3.8 M^{-1}; CaD fragment: Ks=Kd=4.1 M^{-1}; CaD fragment-calmodulin: Ks=Kd=2.2 M^{-1}.

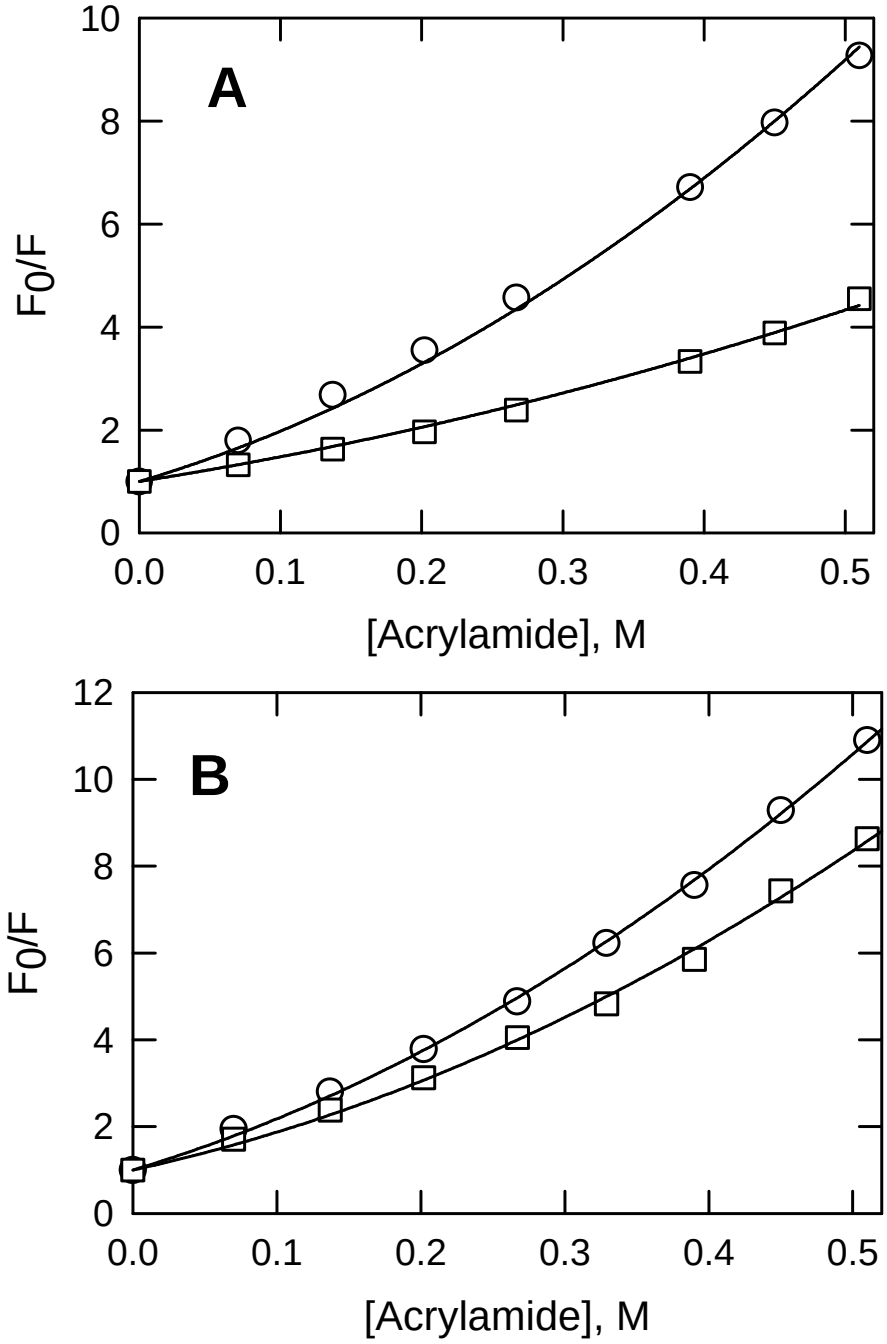
A
B
F_0/F
[Acrylamide], M
0
2
4
6
8
10
12
0.0
0.1
0.2
0.3
0.4
0.5

Analysis of environmental effects on fesselin secondary structure by CD.

Far-UV CD spectroscopy is useful for determining the types of secondary structure present in polypeptide chains. Alpha-helices give characteristic negative peaks near 208 nm and 222 nm and a positive peak around 192 nm, β-sheets yield a negative peak at about 215 nm and a positive peak near 198 nm, and random coils are characterized by a negative peak near 195 nm and by weak ellipticity at 222 nm (Adler et al. 1973).

The CD spectrum of fesselin at 5^{o}C was similar to that of a random coil but the shoulder at 220 nm suggested the presence of some folded secondary structure (Fig 11A). CD spectra of fesselin were recorded at a series of temperatures (Fig 11A-C). With increasing temperature the spectra showed an increase in secondary structure as seen by a less negative peak at 200 nm and appearance of some ellipticity at 220 nm. The greatest amount of structure was seen at 85^{o}C. These temperature effects were totally reversible. It is also noteworthy that the spectra exhibited an isodichroic point near 210 nm, indicating that the temperature-induced transition is two state, from an unfolded structure to a specific more-folded (albeit as yet undetermined) structure.

The CD spectrum of fesselin was insensitive to changes of pH over the range from pH 1.5 to 11.5 (Fig. 11D). The spectra of fesselin were dominated by random coil at all values of pH, although the gain of structure at extreme pH values has been reported for some natively unfolded proteins. This might be explained by the fact that fesselin lacks high net charge typical of many unstructured proteins. High proline content might be the major factor keeping fesselin from folding.

FIGURE 11. Environmental effects on fesselin secondary structure**. A.** Effect of temperature on the structural properties of fesselin. CD spectra of fesselin were measured at increasing temperatures: 5, 15, 25, 35, 45, 55, 65, 75 and 85ºC (in order of the decrease in negative $[\Theta]_{200}$ value, as indicated by the arrow) and cooled down to 5ºC. **B & C.** CD at 222 nm (B) and at 220 nm (C) are reversible with heating (solid lines) and cooling (dashed lines) of fesselin. **D.** CD spectra of fesselin measured at pH 1.5, 3, 5, 6, 7, 8, 11.5.

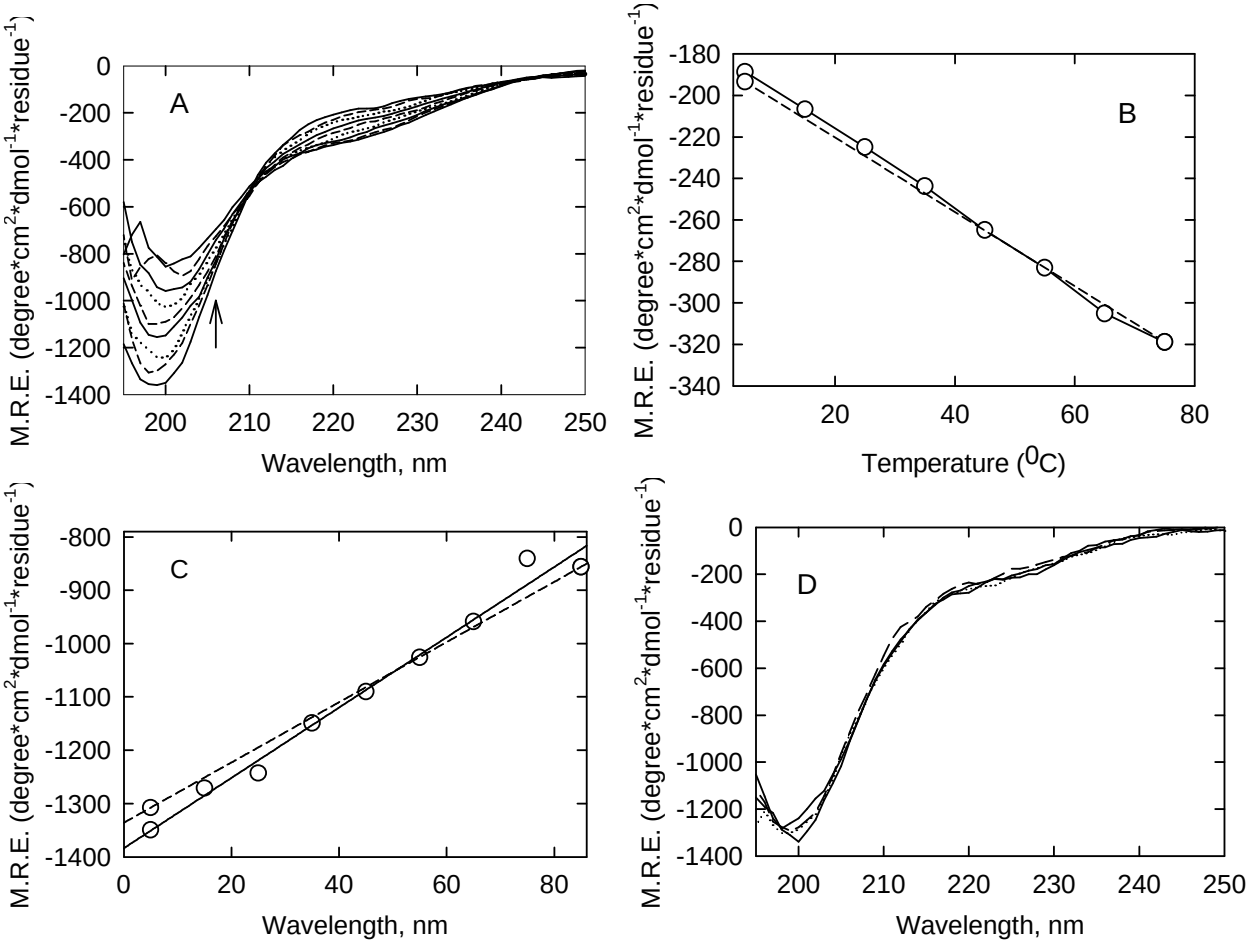
A
B
C
D
M.R.E. (degree*cm^2*dmol^{-1}*residue^{-1})
Wavelength, nm
Temperature (^{0}C)
0
-200
-400
-600
-800
-1000
-1200
-1400
200
210
220
230
240
250
-180
-200
-220
-240
-260
-280
-300
-320
-340
20
40
60
80
-800
-900
-1000
-1100
-1200
-1300
-1400
0

Discussion

Judging from the Stokes radius, the effect of denaturants, the exposure of tryptophan residues to the bulk solvent, the temperature dependence of CD and the insensitivity of CD to changes in pH, fesselin is natively unfolded.

Several structure predictors showed that fesselin (Schroeter et al. 2008) has a predicted structure that consists of unfolded regions interspersed with short structured regions. Such patterns are typical of natively unfolded proteins. These structured regions are known to be important in specific ligand binding in some cases (Mohan et al. 2006; Fuxreiter et al. 2004). The presence of numerous discrete folded regions may account for the ability of fesselin to bind to several ligand proteins.

An analysis of the mean net charge and mean hydrophobicity predicts that avian fesselin falls on the border of unfolded and folded proteins. Fesselin lacks the high net charge at neutral pH typical of many natively unfolded proteins. A high value of net charge at neutral pH causes charge-charge repulsion that prevents natively unfolded proteins from folding (Uversky et al. 2000). The lack of charge repulsion in fesselin explains the insensitivity of the secondary structure of fesselin to changes in pH (Fig. 11D). Fesselin may be unfolded because of the elevated frequency of proline residues in the primary structure. The content of proline residues in the sequence of fesselin is 11.1% while typical globular proteins have a proline content of 4.6% (Tompa, 2002)

The Stokes radius of fesselin was found to be 5.3 nm whereas the expected Stokes radius was about 4 nm. The Stokes radii of natively unfolded proteins are typically larger than predicted for globular proteins of the same molecular weight, that is, unfolded proteins are less compact than

folded proteins. The relationship between Stokes radius and molecular weight of fesselin suggests that fesselin might possess a premolten globule-like conformation. The small amount of secondary structure that we observed by CD spectroscopy is consistent with that conclusion. This residual secondary structure might allow for more efficient folding induced by a binding partner.

Fesselin contains 7 tryptophan residues. 5 residues are found in the disordered regions predicted by the program PONDR (Fig. 6A), and 2 tryptophan residues correlate with the structured units suggested by the Fig. 6A. We observed that the wavelength of the emission maximum of the tryptophan residues in fesselin was close to that of an exposed tryptophan residue. Furthermore, the spectra of fesselin and Cad22 did not change appreciably in the presence of a strong denaturant (6M guanidine HCl) indicating that in both cases most of the tryptophan residues were exposed to solvent. In contrast, the emission spectrum of myosin S1, a known folded protein, was very sensitive to guanidine HCl.

When fesselin was bound to calmodulin, the neutral quencher acrylamide was not able to quench tryptophan fluorescence as effectively as in the case of fesselin alone. This protection could be due to a direct shielding of tryptophan residues by calmodulin or to folding of fesselin upon calmodulin binding. Formation of secondary structure upon ligand binding is known to occur for a number of natively unfolded proteins (Mohan et al. 2006; Oldfield et al. 2005; Bourhis et al. 2004). Molecular recognition elements (MoREs) are able to undergo a disorder-to-order transition that is stabilized by binding to their partner protein or nucleic acid (Mohan et al. 2006; Fuxreiter et al. 2004). We suggest that calmodulin binds to a MoRE of fesselin causing this region to undergo local folding.

Calmodulin had a larger protective effect for Cad22 than for fesselin. This is probably due to the difference in size of fesselin and Cad22. The calmodulin-induced change is probably associated not with the induction of structure at the level of the whole protein, but with the local folding of the region directly involved in binding (Moham et al. 2006; Fuxreiter et al. 2004; Oldfield et al. 2005). Thus the formation of a small folded unit will have a larger impact on a small protein than on a large protein.

Natively unfolded proteins have little secondary structure, but the secondary structure often increases upon heating (Uversky 2002a). At low temperatures fesselin has a typical random coil CD spectrum with some residual secondary structure seen as a small negative shoulder at 220 nm. As the temperature was increased to 85^{o}C this shoulder at 220 nm increased slightly and the peak at 200 nm decreased with the spectra crossing at an isodichroic point (near 210 nm). These changes indicated a transition to a more folded structure at elevated temperatures. The structural changes induced by heating were completely reversible, implying that the unfolded and more-folded structures were in equilibrium. This effect of elevated temperature may be due to increased hydrophobic interactions that are important for folding (Uversky 2002a).

A lot of effort has been made to determine the relationship between intrinsic disorder and biological processes, hence knowledge that fesselin is natively unfolded can be used as a guide for understanding the function of fesselin.

Many proteins involved in cell signaling and molecular recognition are disordered; that enables rapid binding to different targets without sacrificing specificity. For example, the C-terminal domain of C-Fos is intrinsically disordered, nevertheless it is biologically active (Campbell et al, 2000). This

domain activates transcription by interacting with many transcription factors, such as TBP, TFIIH, CBP and Smad3 (Bannister and Kouzarides, 1995; Zhang et al, 1998). Binding to multiple partners is possible due to the conformational freedom of this domain. p53 (Bell et al, 2002) and CREB (Zor et al. 2002) are among other examples of such proteins.

Post-translational modifications often occur in disordered regions, probably due to the ability of such regions to fold onto the surface of enzymes (Dunker et al, 2002). For example, c-src kinase is regulated via tyrosine phosphorylation in its activation loop. When the kinase is inactive the loop is ordered, but it becomes flexible upon kinase activation exposing tyrosine for phosphorylation (Xu et al, 1999b). The majority of phosphorylation sites in p53 are located in its disordered parts (Ayed et al, 2001).

Due to their open structures and ability to interact with multiple partners some natively unfolded proteins regulate the localization of other proteins in the cell by assembling complexes of proteins. Disorder-to-order transition upon binding usually results in formation of tight overall complexes. For example, a scaffold protein caskin has a long unfolded C-terminal domain (Balazs et al, 2009) that can bind to 9 other proteins, and the complex is presumably involved in the assembly of post-synaptic densities.

It is possible that fesselin acts as a potential assembler in smooth muscle cells, because it is localized in the center of actin organization, dense bodies (Renegar et al. 2008), polymerizes and bundles actin (Beall and Chalovich 2001; Schroeter and Chalovich, 2004) and interacts with

other proteins present in dense bodies, such as alpha-actinin (Pham and Chalovich, 2006).

It has been reported that myopodin shuttles between the nucleus and the Z-disks of myocytes depending on its differentiation stage and stress conditions (Weins et al, 2001), and its subcellular localization is controlled by phosphorylation (Faul et al. 2007). Mounting evidence suggests that Z-disks might be actively involved in signaling. Z-disks might function not only by passively transmitting force within myofilaments, but also as a network that can sense changes in mechanical load and communicate the immediate needs of the cell to the nucleus, modifying the pattern of gene expression (Epstein and Davis, 2003; Pyle and Solaro, 2004). Hence it is possible that myopodin/fesselin are involved in signal transduction in the cell.

Fesselin is another example of natively disordered actin-binding proteins, such as caldesmon (Permyakov et al. 2003), thymosin β4 (Czisch et al. 1993), and WASP (Kim et al. 2000). Disorder is thought to correlate strongly with cytoskeletal functions (Xie et al. 2007). The flexible structures of natively unfolded proteins may facilitate actin recognition of a variety of molecular targets, thus explaining the large number of functions attributed to actin.

CHAPTER III. PHOSPHORYLATION OF CALDESMON AT SITES BETWEEN RESIDUES 627-642 ATTENUATES INHIBITORY ACTIVITY AND CONTRIBUTES TO A REDUCTION IN CA^{2+}-CALMODULIN AFFINITY.

We suggested that Ca^{2+}-calmodulin causes the region of fesselin involved in binding to undergo disorder-to-order transition. This idea is supported by our experiments with the whole fesselin molecule, in which we observed a possible increase in the amount of secondary structure of fesselin upon calmodulin binding. Since these conformational changes usually occur locally and the major part of the fesselin molecule probably remains unfolded when Ca^{2+}-calmodulin is bound, studying this induced folding presents a challenge. To overcome this difficulty we tried to clone and express a fragment of fesselin that contains Ca^{2+}-calmodulin binding sites, because the formation of a small folded unit is easier to observe within a small protein than within a large protein. We attempted to express cDNA coding for 10 kD fragment of fesselin containing Ca^{2+}-calmodulin binding sites, either alone or as a fusion with GST or intein (Appendix 1). In no case did we observe a detectable amount of expression. It is possible that the 10 kD fesselin fragment is highly disordered and hence subject to rapid proteolytic degradation in the cell.

Since our attempt to make a fragment of fesselin failed, we wanted to use a C-terminal fragment of caldesmon to determine whether phosphorylation of natively unfolded actin binding proteins causes structural and functional changes similar to those observed by ligand binding.

Caldesmon, another natively unfolded protein that is regulated by Ca^{2+}-calmodulin and phosphorylation, is an important regulator of smooth

muscle contraction and shares numerous functions with fesselin, as reviewed in the Introduction. Ca^{2+}-calmodulin binding causes formation of a local structure in the unfolded C-terminal region of caldesmon (Permyakov et al. 2003; Zhou et al; 1997). Although it is known that phosphorylation functionally affects caldesmon in a way similar to Ca^{2+}-calmodulin, i.e. both reduce its actin-binding affinity and release the inhibition of the actomyosin ATPase activity by caldesmon, very little is known about the effect of phosphorylation on the structure of caldesmon. It might be possible that phosphorylation of caldesmon causes a conformational change that mimics its Ca^{2+}-calmodulin binding state.

There are examples of other natively unfolded proteins that increase their secondary structure upon phosphorylation. For example, a protein Tau that is related to Alzheimer's disease is hyperphosphorylated in its pathological state. Its ability to form alpha-helices, which has been associated with pathological protein aggregation, increases with phosphorylation (Mendieta et al. 2005).

We wanted to explore the possibility that phosphorylation of the natively unfolded caldesmon C-terminus causes structural changes similar to those observed upon Ca^{2+}-calmodulin binding.

We used CaD22 phosphorylated with PAK as a model because (i) PAK was shown to phosphorylate caldesmon *in vivo* (Eppinga et al. 2006), (ii) constitutively active PAK3 produces Ca^{2+}- independent contraction of smooth muscle that coincides with an increase in caldesmon phosphorylation (Van Eyk et al. 1998) and (iii) PAK appears to be an important regulator of caldesmon-mediated actin dynamics (Eppinga et al. 2006; Dharmawardhane et al, 1997) and cell motility (Jiang et al. 2010) *in vivo*.

Results

Effect of PAK phosphorylation and calmodulin binding on the amount of secondary structure in caldesmon.

Far UV CD spectroscopy was used to monitor the amount of secondary structure in CaD22. Figure 12A represents the CD spectra of CaD22 before and after incubation with PAK. No appreciable difference was recorded between the unphosphorylated and phosphorylated CaD22. This suggests that phosphorylation of caldesmon by PAK does not cause any significant changes in the secondary structure of caldesmon, unlike Ca^{2+}-calmodulin binding, as described by Permyakov et al. 2003. As a control we reproduced the CD spectra for CaD22, calmodulin and CaD22-calmodulin complex as described in Permyakov et al 2003 (Figure 12B). We compared the measured and the calculated spectra for CaD22 alone and in complex with calmodulin. If calmodulin binding does not induce any structural changes in caldesmon then the measured spectrum should be equal to the calculated one. However, if calmodulin binding does induce structural changes then the measured and the calculated spectra will be different. Figure 12B shows that the experimentally measured spectrum of CaD22 alone (solid line) is different from the calculated spectrum of CaD22 when bound to calmodulin (dashed-dotted line), as seen by Permyakov et al 2003. CaD22 alone produces a spectrum typical of natively unfolded proteins with an intense negative peak in the 200 nm region and a weak signal in the vicinity of 222 nm. The calculated spectrum for CaD22 bound to calmodulin shows less intense minimum at 200 nm and increased negative intensity near 222 nm, suggesting the increase in the ordered

secondary structure. Hence PAK phosphorylation and Ca^{2+}-calmodulin binding to CaD22 do not cause similar structural changes in caldesmon.

To ensure that CaD22 was indeed phosphorylated by PAK we compared migration of unphosphorylated and phosphorylated CaD22 on isoelectric focusing gels (Figure 13). PAK kinase was shown to phosphorylate caldesmon at two sites, Ser 672 and Ser 702 and phosphorylation was complete within the course of 1.5-2 hours. (Foster et al. 2000). Figure 13A shows untreated CaD22 (lane 1) and CaD22 that was treated with PAK for 1.5 hours (lane 2) and 20 hours (lane 3). Untreated CaD22 focused as 2 closely spaced bands. The number of bands with lower isoelectric points increased after 1.5 hours of incubation with PAK, as expected. Surprisingly, we observed a further increase in the number of bands with lower isoelectric points after 20 hours of incubation. SDS gels showed that the CaD22WT remained intact during those periods of incubation (Figure 13B). These time dependent shifts raised the possibility that more than 2 sites within CaD22 became phosphorylated. We wanted to investigate the effects of the additional phosphorylation on the properties of caldesmon.

Figure 12. PAK phosphorylation does not significantly affect the secondary structure of caldesmon. A. Far UV CD spectra of CaD22 before (solid line) and after (dashed line) phosphorylation by PAK. B. Far UV CD spectra of CaD22 (solid line), calmodulin (dashed-double dotted line) and CaD22-calmodulin complex (dotted line). The molar ratio of CaD22:calmodulin was 1:1. Spectrum of CaD22 bound to calmodulin was calculated as ((CaD22-CaM)-(1/2CaM)) and shown as a dashed-dotted line. The conditions were 50 mM potassium chloride, 2 mM sodium phosphate and 2 mM $CaCl_2$ at 20^{o}C. M.R.E. – mean residue ellipticity.

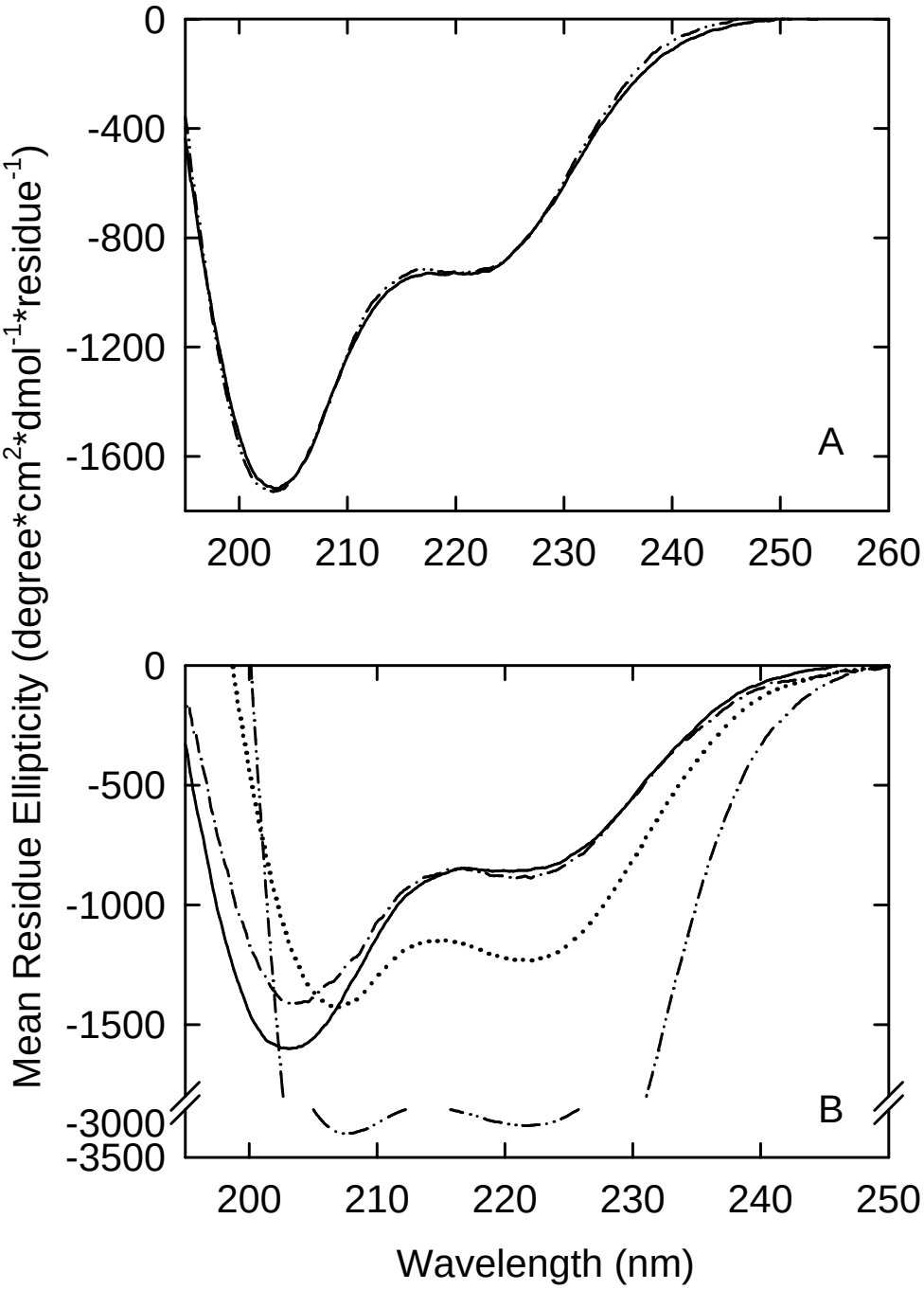
0
-400
-800
-1200
-1600
A
200
210
220
230
240
250
260
0
-500
-1000
-1500
-3000
-3500
B
200
210
220
230
240
250
Wavelength (nm)
Mean Residue Ellipticity (degree*cm-2*dmol-1*residue-1)

Figure 13. PAK phosphorylation changes charge in CaD22.

A. Non-equilibrium isoelectric focusing gel. Lane 1: CaD22WT, Lane 2: CaD22WT PAK phosphorylated for 1.5 hours, Lane 3: CaD22WT after PAK phosphorylation for 20 hours. B. SDS-gel. Lane 1: CaD22WT, Lane 2: CaD22WT after PAK phosphorylation for 20 hours.

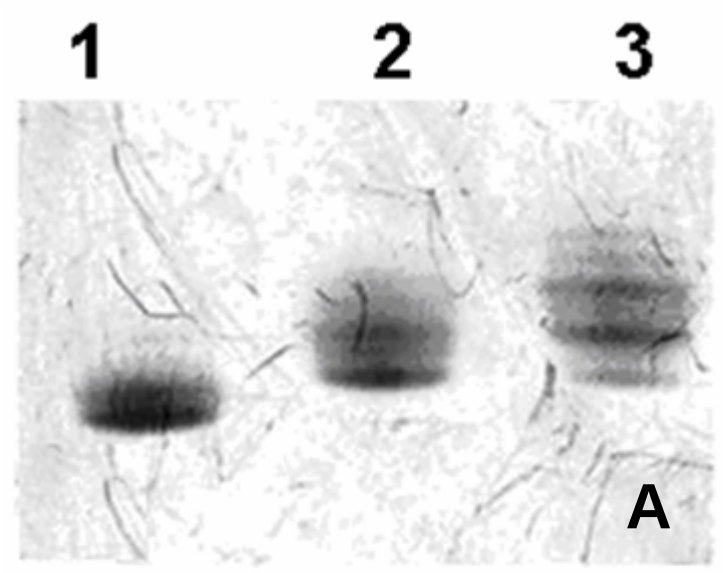
1
2
3
A

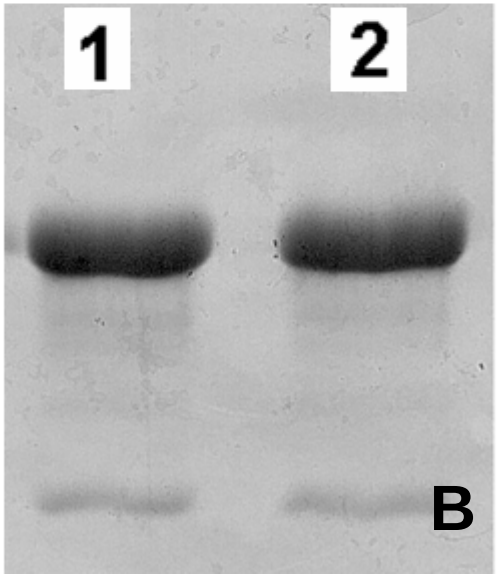
1
2
B

No-phosphorylation and constitutive phosphorylation-mimicking mutants.

To study the effects of additional phosphorylation of CaD22 by PAK we modified the two major phosphorylation sites, Ser672 and Ser702 of chicken gizzard CaD22. Serine to alanine substitutions were made to mimic the non-phosphorylated state (CaD22AA). The phosphorylated state was mimicked by replacing both serine residues with aspartic acid residues (CaD22DD). The presence of the correct mutations was verified by sequencing both plasmids. For wild type CaD22 the observed mass (22625 Da) was consistent with the calculated mass (22630 Da). Similar agreement was obtained for the observed mass (22690 Da) and calculated mass (22686 Da) of CaD22DD. In both cases the observed masses were within 0.02% of the calculated ones.

The presence of additional charges in the CaD22DD mutant was verified by nonequilibrium isoelectric focusing gels. Theoretical pI values for CaD22 and CaD22DD are 9.7 and 9.56, respectively. Figure 14A shows that CaD22DD (lane 2) migrated less toward the cathode than wild type CaD22 (lane 1). The migration of the AA mutant was identical to the wild type (not shown). CaD22WT, CaD2AA and CaD22DD migrated similarly on SDS gels (data not shown).

Analysis of the time course of CaD22 phosphorylation by PAK by isoelectric focusing gels.

To test the possibility that PAK phosphorylates residues other than Ser672 and Ser 702 on caldesmon, the two types of CaD22 that lacked phosphorylation sites at 672 and 702 were subjected to PAK treatment. Fig. 14B shows CaD22DD before (lane 3) and after (lane 4) a 20 hour

incubation with PAK. Fig. 14C shows CaD22AA before (lane 5) and after (lane 6) a 20 hour incubation with PAK. The additional acidic bands present in both cases indicated that additional phosphorylation sites were present.

Analysis of the time course of CaD22 phosphorylation by PAK by measuring the incorporation of ^{32}P into caldesmon.

Figure 15 shows the time courses of phosphorylation of wild type and CaD22AA by PAK. CaD22WT was phosphorylated to give 2 mol phosphate/mol CaD22 (open circles) in the first phase. Upon continued incubation the caldesmon fragment slowly incorporated additional phosphate residues giving 3.3 mol phosphate/mol CaD22 after 23 hours. When the study was repeated with CaD22AA having the two major PAK sites blocked, the first phosphorylation phase was absent, but the additional slow phosphorylation still occurred (solid circles).

Figure 14. Non-equilibrium isoelectric focusing showing charge changes in CaD22 following PAK phosphorylation. (A) Lane 1: CaD22WT, Lane 2: CaD22DD. (B) Lane 3: CaD22DD, Lane 4: CaD22DD after incubation for 20 hours with PAK. (C) Lane 5: CaD22AA, Lane 6: CaD22AA after incubation for 20 hours with PAK.

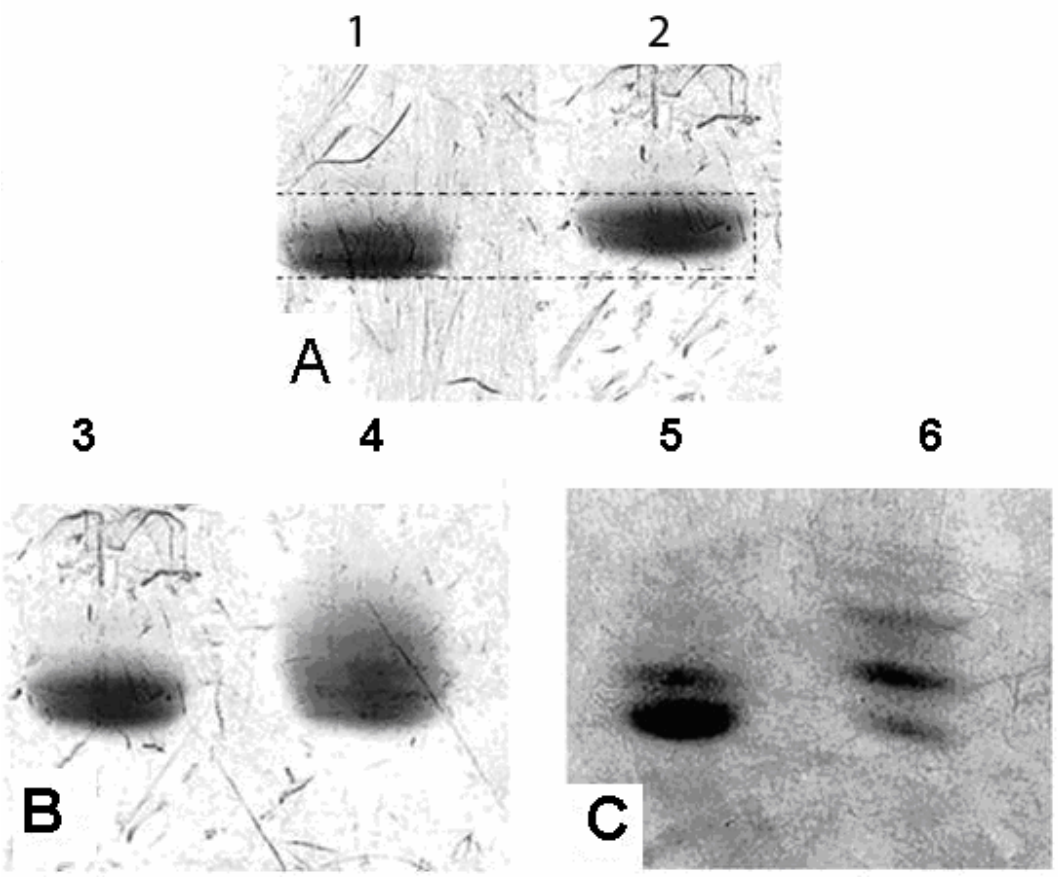
1
2
A
3
4
5
6
B
C

Figure 15. Two sets of sites on CaD22 were phosphorylated by extended treatment with PAK. The phosphorylation time course was followed by ^{32}Pi incorporation at 25℃ in a buffer containing 20 mM Tris-HCl pH 7.5, 100 mM NaCl, 5 mM $MgCl_2$, 1 mM DTT and 1 mM ^{32}P-ATP ($4x10^5$ cpm/nmol). Both CaD22WT (open circles) and CaDAA (solid circles) are shown. Phosphorylation at sites other than Ser672 and Ser702 is evident in both cases.

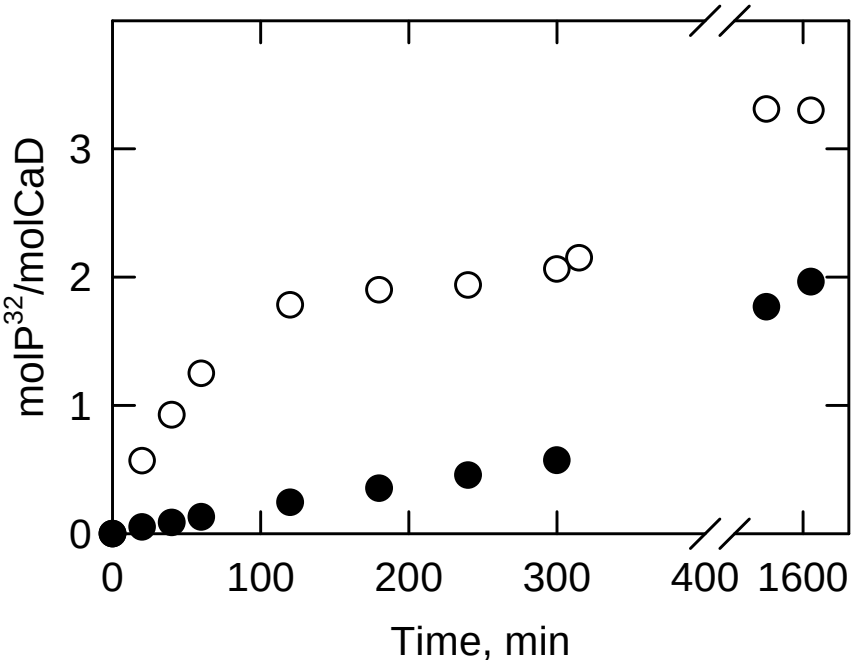
molP32/molCaD
0
1
2
3
0
100
200
300
400
1600
Time, min

Effect of phosphorylation at the major and minor sites of CaD22 on Ca^{2+}-calmodulin binding.

The effect of phosphorylation at the major and minor sites of CaD22 on Ca^{2+}-calmodulin binding was determined with intrinsic tryptophan fluorescence measurements. Figure 16 compares Ca^{2+}-calmodulin binding isotherms for CaD22 that was non-phosphorylated, phosphorylated only at the major sites and phosphorylated at both the major and minor sites. Phosphorylation at the major sites reduced the affinity of CaD22 for Ca^{2+}-calmodulin from K_d=0.11 μM (open circles) to K_d=0.8 μM (dotted circles). More extensive phosphorylation (solid circles) caused further reduction in the binding affinity, to about 4.0 μM. An examination of the 95% confidence limits shows that the three binding curves are statistically different.

The study of Figure 16 was repeated with mutants of CaD22 lacking the major phosphorylation sites. CaD22AA lacks charges at the major sites and cannot be phosphorylated at these sites. Figure 17A compares unphosphorylated CaD22AA with CaD22AA that was treated with PAK for up to 20 hours. Although such treatment caused phosphorylation at the minor sites the affinity for Ca^{2+}-calmodulin was unaffected. The affinities of both phosphorylated and non-phosphorylated CaD22AA for Ca^{2+}-calmodulin were similar to that of the wild type CaD22 (Fig. 17A). That is, curves for both phosphorylated and non-phosphorylated CaD22AA fell within the 95% confidence interval for the wild type curve. On the other hand, CaD22DD bound weaker to Ca^{2+}-calmodulin than CaD22WT, but not as weak as CaD22-PAK. That is, the 95% confidence intervals did not overlap. The curve for phosphorylated CaD22 from Fig. 16 is shown for comparison (dashed curve).

CaD22DD has negative charges at the major sites and incubation with PAK led to phosphorylation of only the minor sites. Treatment of CaD22DD with PAK caused further reduction in the binding affinity, bringing it close to that of the phosphorylated wild type CaD22 (Fig. 17B).

The results of Fig. 17 suggest that phosphorylation of caldesmon at the unknown sites affects Ca^{2+}-calmodulin binding only if the two major PAK sites are already phosphorylated.

Figure 16. Phosphorylation at both the major and minor sites of CaD22 decreased the affinity to Ca^{2+}-calmodulin. Binding was measured to CaD22 (open circles), CaD22 treated for 1.5 hours (dotted circles) and CaD22 treated for 20 hours with PAK (solid circles). The data shown are from 4, 1 and 3 data sets, respectively. The data were globally fit. The dotted lines represent 95% confidence intervals for each curve. Phosphorylation at the major sites (dotted circles) reduced the affinity from 0.11 μM to 0.8 μM. Additional phosphorylation to give 3.3 Pi/caldesmon reduced the affinity to 4.0 μM. Inset: Plot of fraction of maximum binding against log[CaM_{free}]. The reaction buffer contained 10 mM MOPS pH 7.2, 100 mM NaCl, 1 mM DTT, 2 mM $CaCl_2$ at 20^{o}C. CaD22 concentration was 0.6 μM.

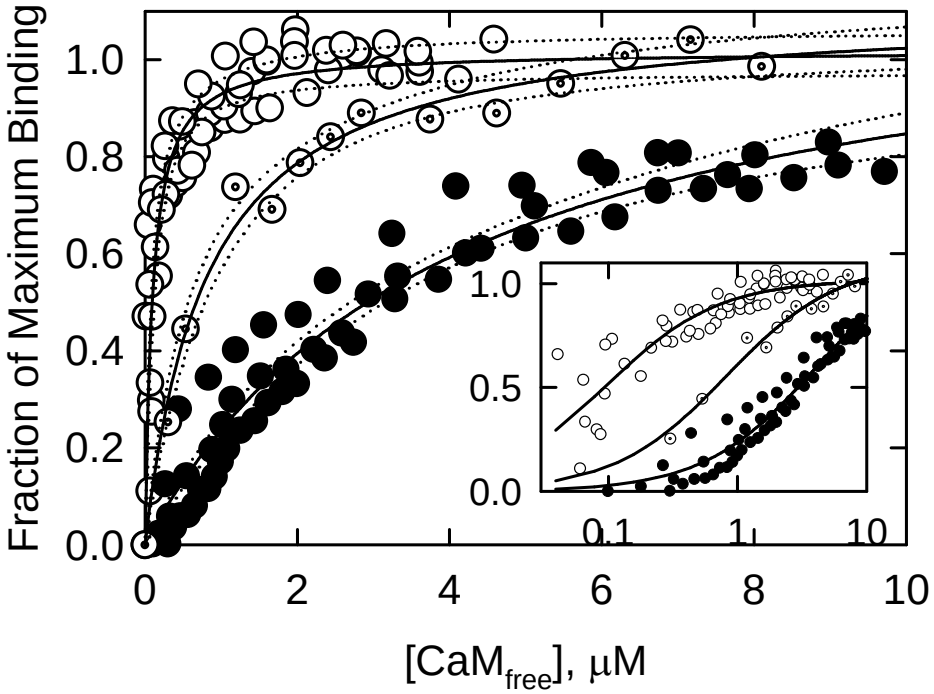
Fraction of Maximum Binding
1.0
0.8
0.6
0.4
0.2
0.0
0
2
4
6
8
10
[CaM$_{free}$], μM
1.0
0.5
0.0
0.1
1
10

Figure 17. Effect of phosphorylation at the minor sites of CaD22AA (A) and CaD22DD (B). CaD22 decreased calmodulin binding only if the major sites were negatively charged. (A) Binding to CaDAA (open triangles, 4 data sets) was identical to that of wild type (open circles, 4 data sets) and was unaffected by PAK treatment for 20 hours (solid triangles, 3 data sets). Phosphorylation of CaD22AA increased the affinity for Ca^{2+}-calmodulin slightly (K_d decreased from 0.1 μM to 0.04 μM). The inset shows the fraction of maximum binding versus log[CaM_{free}]. (B) Substituting PAK phosphorylation sites with Asp, i.e. CaD22DD, (open triangles, 3 data sets) reduced the affinity of CaD22 to Ca^{2+}-calmodulin to 1.15 μM compared with 0.1 μM for wild type unphosphorylated (open circles, 4 data sets). Incubation of CaD22DD with PAK for 20 h (solid triangles, 3 data sets) caused a further reduction in its affinity of binding to calmodulin to 3.1 μM. The dotted lines represent 95% confidence intervals for each curve. Conditions are the same as in Fig. 16.

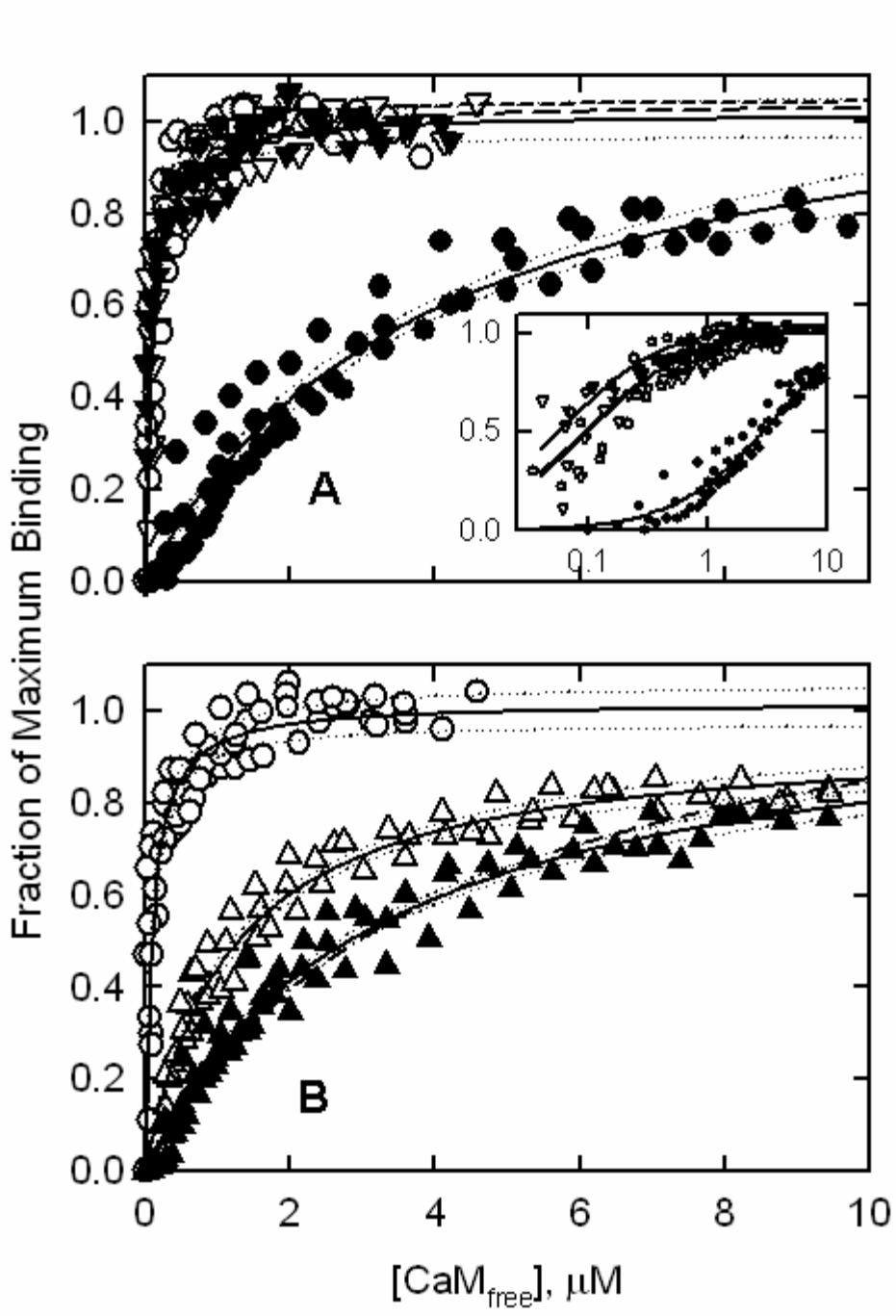
Fraction of Maximum Binding
1.0
0.8
0.6
0.4
0.2
0.0
A
1.0
0.5
0.0
0.1
1
10
B
0
2
4
6
8
10
[CaM$_{free}$], μM

Effect of phosphorylation at the major and minor sites of CaD22 on the stoichiometry of binding to calmodulin.

Phosphorylation of CaD22 may have altered the stoichiometry of binding to calmodulin in addition to decreasing the stability of the interaction. The stoichiometry was determined by repeating binding studies at CaD22 concentrations that exceeded the dissociation constant for the CaD22-calmodulin complex (Figure 18). As the concentration of calmodulin was increased a plateau of binding was reached at the same ratio of calmodulin to caldesmon for all of the CaD constructs. CaD22 formed 2:1 complexes with Ca^{2+}-calmodulin in agreement with previously reported data (Medvedeva et al. 1997).

Analysis of the effect of Ca^{2+}-calmodulin on the time course of phosphorylation of the minor sites.

Because phosphorylation of caldesmon by PAK on the minor sites affected binding to Ca^{2+}-calmodulin, we measured the effect of Ca^{2+}-calmodulin on the time course of phosphorylation of CaD22AA by PAK (Figure 19). In the presence of Ca^{2+}-calmodulin (open squares) the phosphorylation of the minor sites was significantly slower that in the absence of Ca^{2+}-calmodulin (open triangles). PAK did not phosphorylate Ca^{2+}-calmodulin significantly (open circles).

Figure 18. The stoichiometry of CaD22 binding to calmodulin was altered neither by the DD mutation nor by PAK phosphorylation. CaD22 WT (open circles), WT-PAK (solid circles), DD (open triangles) and DD-PAK (solid triangles) were titrated with Ca^{2+}-calmodulin. The CaD22 concentration was 20 μM which is greater than the weakest dissociation constant (i.e. 4 μM for PAK phosphorylated CaD22). Under these conditions all added calmodulin bound to the CaD22 thus defining the stoichiometry under these conditions (2 mol CaD22 per mol calmodulin).

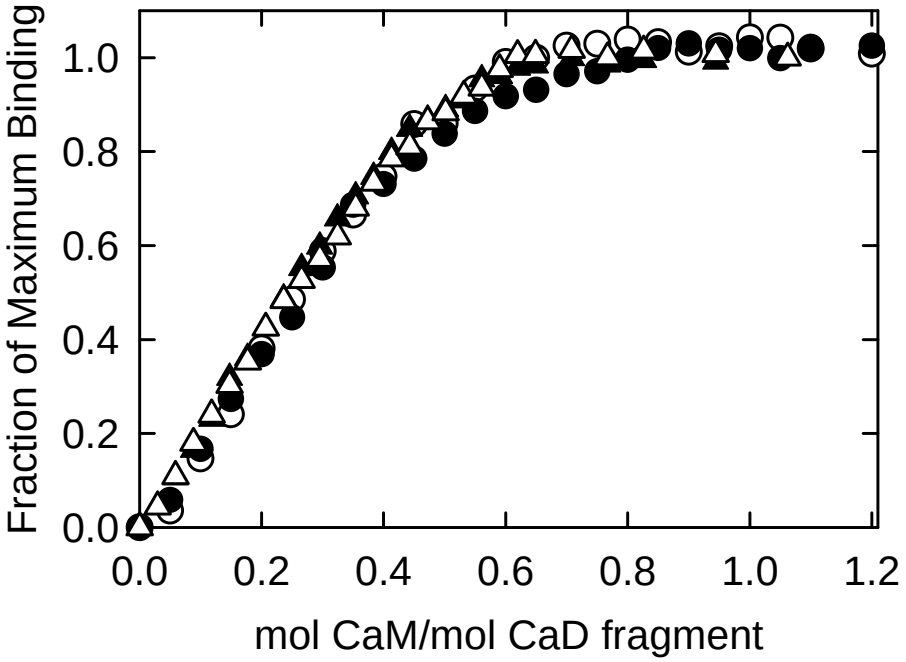
Fraction of Maximum Binding
0.0
0.2
0.4
0.6
0.8
1.0
0.0
0.2
0.4
0.6
0.8
1.0
1.2
mol CaM/mol CaD fragment

Figure 19. Ca^{2+}-calmodulin binding decreased the rate of phosphorylation of the minor sites by PAK. Phosphorylation time courses were measured as described in Figure 2 with 0.5 μM CaD22AA and 2 μM Ca^{2+}-calmodulin. Phosphorylation time courses of CaD22AA in the absence (open triangles) and in the presence of Ca^{2+}-calmodulin (open squares) are shown. Ca^{2+}-calmodulin was not appreciably phosphorylated by PAK (open circles).

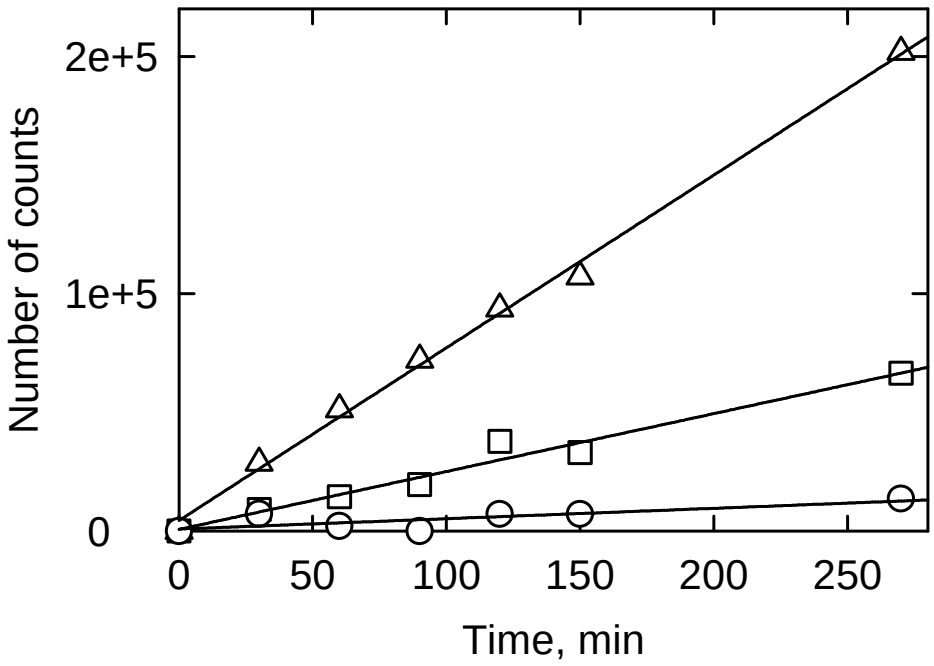
2e+5
1e+5
0
Number of counts
0
50
100
150
200
250
Time, min

Effect of phosphorylation at the major and minor sites of CaD22 on the ability of caldesmon to inhibit actin-activated myosin S1 ATPase activity.

Phosphorylation of caldesmon reduces the ability of caldesmon to inhibit actin-activation of myosin S1 ATPase activity. We examined the contribution of the major and minor PAK phosphorylation sites on the inhibitory activity of CaD22. Figure 20A shows the rate of actin activated ATPase activity as a function of wild type CaD22. The CaD22 had produced inhibition that was typical of caldesmon. In particular, tropomyosin markedly enhanced the inhibitory activity of CaD22.

CaD22AA was expected to behave like wild type CaD22. As shown in Fig 20B CaD22AA had the same inhibitory activity as wild type CaD22 (Fig. 20B open triangles down and open circles). The mutant designed to mimic phosphorylation at sites 672 and 702 was expected to have a diminished inhibitory activity. However, CaD22DD (Fig. 20B open triangles up) had the same inhibitory activity as wild type and CaD22AA. After overnight incubation with PAK, the mutants as well as wild type CaD22 had similarly reduced inhibitory activities (Fig.20B, closed symbols). Because the minor sites were not totally phosphorylated the total extent of reversal of activity was not determined. These results suggested that the introduction of negative charges into the minor sites but not the major sites attenuated the inhibitory activity of CaD22.

We also examined the effects of negative charges at sites 672 and 702 in a larger caldesmon construct, CaD35. That construct was previously characterized in our laboratory (Fredricksen et al. 2003). The inset in Fig. 20B shows that CaD35DD had the same ability to inhibit actin stimulated ATPase activity as CaD35WT.

Figure 20. Phosphorylation of the minor sites of CaD22 reduced the inhibition of actomyosin ATPase activity. (A) Control showing actin-activated S1-ATPase activity as a function of CaD22WT in the absence (open circles) and presence (solid circles) of smooth muscle tropomyosin. Concentrations of actin, smooth muscle tropomyosin and myosin S1 were 10 μM, 2.2 μM and 0.1 μM, respectively. The final solution composition was 1 mM ATP, 3 mM $MgCl_2$, 31 mM NaCl, 10 mM imidazole pH 7.0 at 25℃. (B) Actin-activated S1-AT Pase as a function of phosphorylated and unphosphorylated CaD22WT (circles), CaD22DD (triangles up) and CaD22AA (triangles down). Open symbols show the effect of unphosphorylated CaD22 whereas solid symbols show the corresponding species after 20 hour treatment with PAK. The inset shows actin-activated S1-ATPase as a function of CaD35WT and CaD35DD.

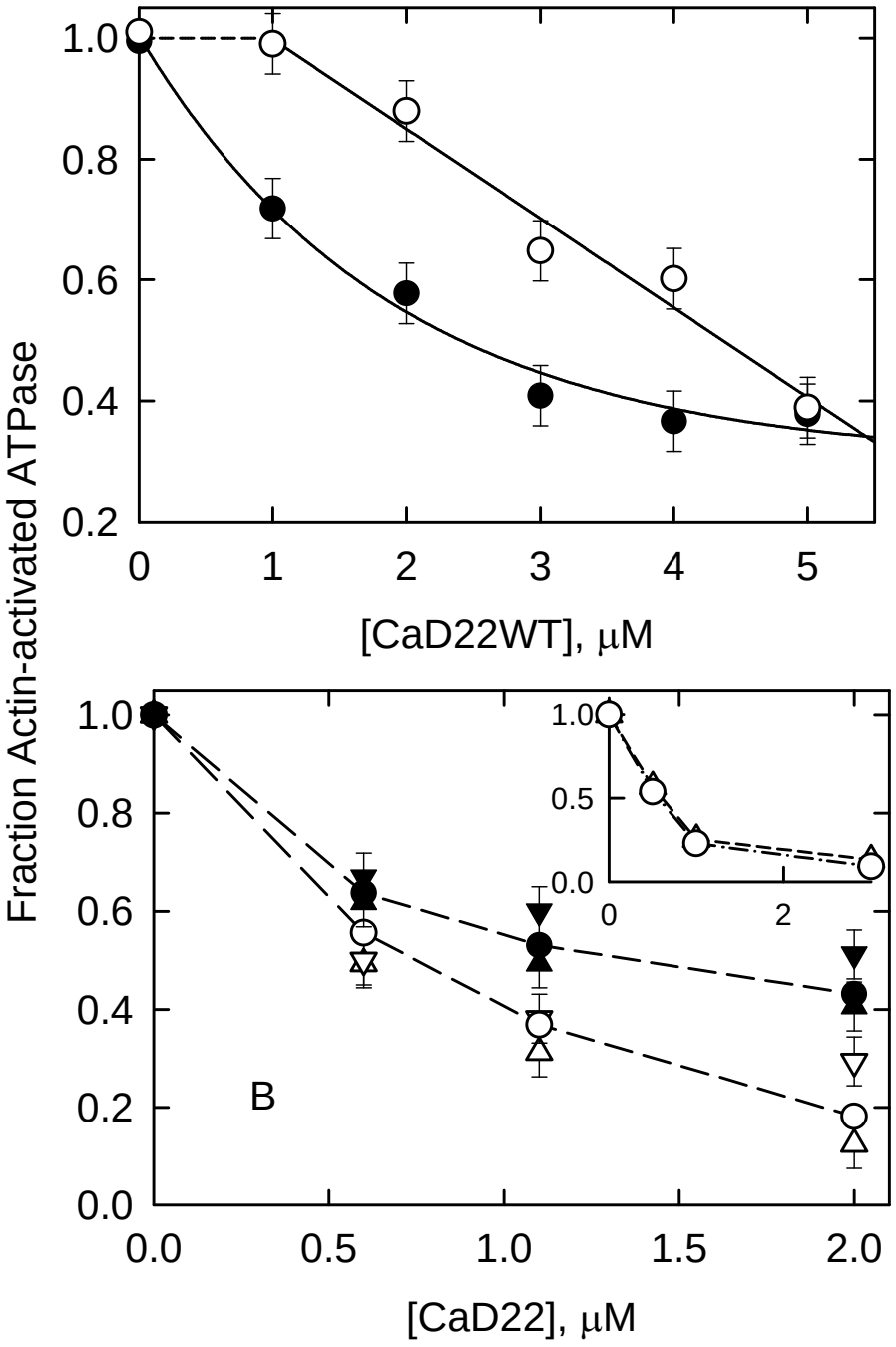
Fraction Actin-activated ATPase
1.0
0.8
0.6
0.4
0.2
0
1
2
3
4
5
[CaD22WT], μM
1.0
0.8
0.6
0.4
0.2
0.0
0.0
0.5
1.0
1.5
2.0
B
1.0
0.5
0.0
0
2
[CaD22], μM

Analysis of the calmodulin dependencies of ATPase activities of unphosphorylated and phosphorylated caldesmon.

The results of Figures 16 and 20 indicate that phosphorylation of CaD22 may have more significant effects on ATPase activity in the presence of Ca^{2+}-calmodulin. That possibility was investigated by comparing the calmodulin dependencies of ATPase activities of unphosphorylated and phosphorylated CaD22. Ca^{2+}-calmodulin was effective in reversing CaD22WT inhibition of actomyosin ATPase (Figure 21, open circles), but was not able to effectively reverse the inhibition by CaD22DD in which only the major PAK sites were negatively charged (open triangles). That is, when the major PAK sites were negatively charged caldesmon was inhibitory even in the presence of Ca^{2+}-calmodulin. When CaD22 was phosphorylated at both the major and minor sites with PAK there was less inhibition of ATPase activity in the absence of Ca^{2+}-calmodulin and Ca^{2+}-calmodulin had little effect on the degree of inhibition.

Identification of the minor PAK phosphorylation sites in CaD22.

The additional sites of phosphorylation of CaD22 were identified by mass spectrometry. CaD22WT and CaD22WT incubated with PAK for 20 hours were digested with modified trypsin and analyzed by LC-MS/MS, as described in Materials and Methods. The phosphorylated peptides and corresponding non-phosphorylated peptides were compared. The phosphorylated residues corresponded to Thr627, Ser631, Ser635 and Ser642. Phosphorylated Thr627 and Ser631 were the most abundant. The localization of these sites relative to other known phosphorylation sites is shown in Figure 22.

Figure 21. Ca^{2+}-calmodulin has different effects on the inhibitory activities of unphosphorylated and highly phosphorylated CaD22. Shown are unphosphorylated CaD22WT (open circles), CaD22WT-PAK incubated with PAK for 20 hours (solid circles) and CaD22-DD (open triangles). Conditions are the same as in Fig. 20 except [CaD22] was held constant at 1.1 μM.

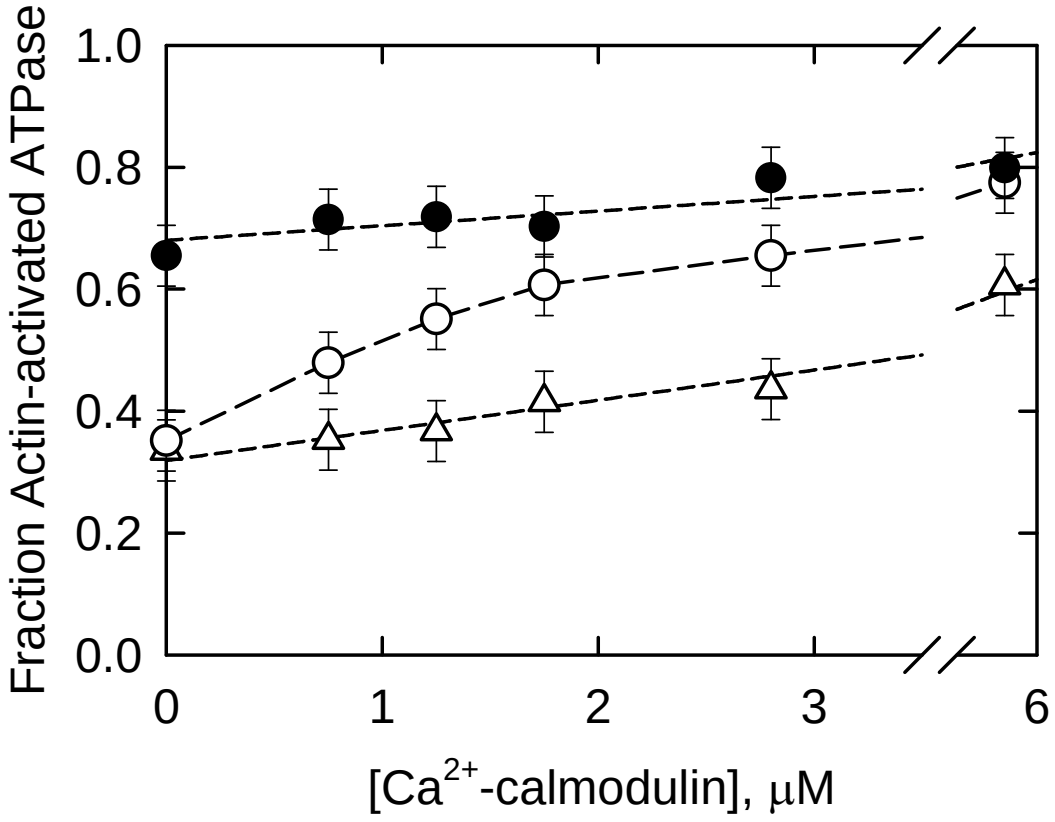
Fraction Actin-activated ATPase
1.0
0.8
0.6
0.4
0.2
0.0
0
1
2
3
6
[Ca2+-calmodulin], μM

Figure 22. Phosphorylation sites on CaD22. All phosphorylation sites are in bold. Major PAK kinase sites are in square brackets. Minor PAK sites are in parentheses. MAPK sites[1], Calmodulin kinase II sites[2], cdc2 kinase sites[3] and PKC sites[4] are indicated with superscripts as shown. The tropomyosin-binding region has a single underline. The calmodulin-binding regions have a double underline. The residue numbers at the beginning and at the end of the sequence are in curly brackets.

{563}MKEEIERRRAEAAEKRQKVPEDGVSEEKKPFKCFS[3]PKGS**S**[2,4]LKIEERAEFLNK

SAQKSGMKPAHT(**T**)AVV(**S**)KID(**S**)[2]RLEQYT(**S**)AVVGNKAAKPAKPAASDLPVPAE

GVRNIK[**S**]MWEKGNVFSS[3]PGGTGT[3]PNKETAGLKVGVS[**S**]RINEWLTKT[3]PEGNK**S**[1,3]

PAPKPSDLRPGDVSGKRNLWEKQ**S**[2,4]VEKPAASSSKVTATGKKSETNGLRQFEKEP{771}

Analysis of the contribution of one of the minor PAK sites, Thr627.

It is not clear whether all of the minor sites, a combination of these sites or just one of them is responsible for the observed functional effects. We modified Thr 627 to Asp in CaD22DD to mimic the phosphorylated state of that minor site and the 2 major sites

The sequences of the DNA and mutant were verified. The observed mass difference between the triple mutant and the wild type caldesmon (68) agreed with the calculated difference (70).

Figure 23 shows the effect of phosphorylation of Thr627 and the major sites on binding to Ca^{2+}-calmodulin, The affinity of the triple mutant for Ca^{2+}-calmodulin was weaker than that for CaD22WT (open circles), but stronger than that of CaD22-PAK (dashed line). The binding affinity of the triple mutant was similar to that of CaD22DD that has negative charges on the major sites only. Treatment of the triple mutant with PAK reduced the binding affinity, bringing it close to that of the phosphorylated wild type CaD22. This suggests that the residue Thr627 by itself does not affect Ca^{2+}-calmodulin binding to caldesmon phosphorylated on the major sites.

Figure 23. Aspartate substitution at Thr627 in combination with aspartate substitutions at the major sites did not affect calmodulin binding. Calmodulin binding curves for wild type (open circles, 4 data sets), triple mutant (open diamonds, 3 data sets) and triple mutant after 20 h PAK treatment (solid diamonds, 2 data sets) are shown with their 95% confidence limits (dotted lines). Dissociation constants for CaD22DD and the triple mutant were 1.15 μM and 1.64 μM, respectively. The binding curve for the triple mutant was similar to that of CaD22DD (short dashed line). PAK phosphorylation of the triple mutant reduced the affinity to 4.5 μM which is similar to that observed for CaD22WT-PAK (long dashed line). Conditions are the same as in Fig. 16.

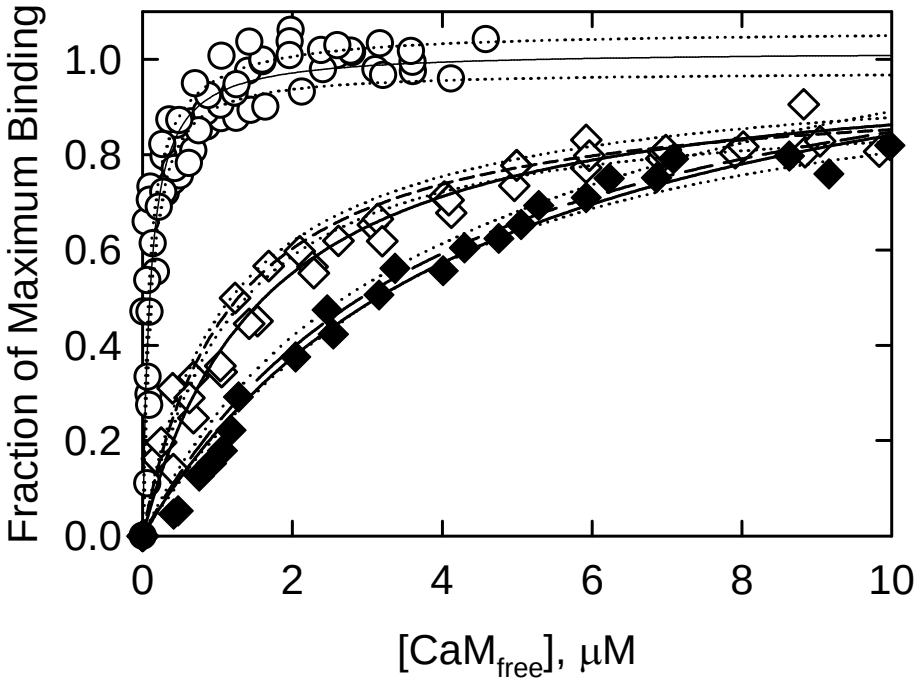
Fraction of Maximum Binding
1.0
0.8
0.6
0.4
0.2
0.0
0
2
4
6
8
10
[CaM$_{free}$], μM

Because of the role of phosphorylation of the minor sites in controlling inhibition of ATPase activity by caldesmon (Figure 20) we explored the effects of the triple mutant on the ATPase activity of caldesmon. The triple mutant (Figure 24, open diamonds) had the same inhibitory activity as the wild type CaD22 (open circles) and did not exhibit the reduced inhibitory activity, as the wild type phosphorylated by PAK on both the major and the minor residues (Figure 20B).

Figure 24. Aspartate substitution at Thr627 in combination with aspartate substitutions at the major sites did not affect the inhibition of actomyosin ATPase activity by caldesmon. Actin-activated S1-ATPase rates are shown as a function of concentrations of unphosphorylated CaD22WT (open circles) and the triple mutant (open diamonds). Conditions are the same as in Figure 20.

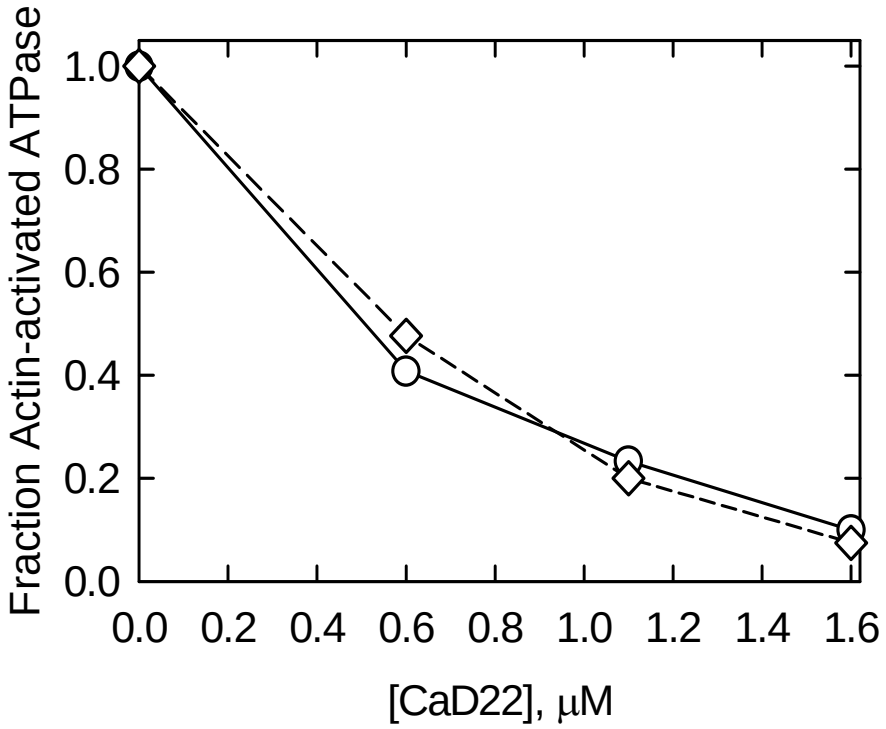
Fraction Actin-activated ATPase
1.0
0.8
0.6
0.4
0.2
0.0
0.0
0.2
0.4
0.6
0.8
1.0
1.2
1.4
1.6
[CaD22], μM

Discussion

PAK kinase phosphorylates caldesmon at Ser 672 and Ser 702 (Foster et al. 2000). Phosphorylation at these sites reduces binding to calmodulin and gives a partial reversal of the inhibitory action of caldesmon on actomyosin ATPase activity (Foster et al. 2000; Eppinga et al. 2006). We confirmed the effect of phosphorylation on calmodulin binding but we observed little change in ATPase inhibitory activity. Phosphorylation at Thr627, Ser631, Ser635, and Ser642 further weakened calmodulin binding and partially reversed ATPase activity. Serine residues at sites 672 and 702 were substituted with either aspartic acid (CaD22DD) or alanine (CaD22AA) to simulate the phosphorylated and non-phosphorylated states, respectively. This procedure permitted us to investigate the relationship among the major (672, 702) and minor (627, 631, 635, and 642) sites of phosphorylation.

In the case of phosphorylated wild type CaD22 the affinity for Ca^{2+}-calmodulin decreased after further incubation with PAK. That further incubation was accompanied by phosphorylation at the minor sites. To insure that the further reduction in affinity was not linked to an increase in phosphorylation of the major sites we utilized CaD22DD. The affinity of CaD22DD for Ca^{2+}-calmodulin was about 10% of that observed with wild type CaD22. Incubation of CaD22DD with PAK caused a further reduction in affinity for Ca^{2+}-calmodulin to about 3% of the wild type affinity. The effect of phosphorylation of the minor sites on Ca^{2+}-calmodulin binding was dependent on the prior phosphorylation of the major sites. Replacement of serine residues 672 and 702 by alanine had no effect on Ca^{2+}-calmodulin binding compared to wild type CaD22. Incubation of CaD22AA with PAK did not weaken Ca^{2+}-calmodulin binding although the minor sites became

phosphorylated. That is, the only effect of phosphorylation of the minor sites on Ca^{2+}-calmodulin binding is to enhance the effect of phosphorylation at the major sites.

The effect of phosphorylation at the major PAK sites on weakening Ca^{2+}-calmodulin binding is easy to rationalize because those sites are adjacent to the Ca^{2+}-Calmodulin binding region of calmodulin. However, the minor phosphorylation sites are about 30 residues upstream from the closest known calmodulin binding site (Fig. 22). One hypothesis for such a change is that calmodulin binding induces structural changes in the natively unfolded C-terminal region of caldesmon. Flexation of caldesmon peptide chain in the C-terminal region resulting in multiple contacts with calmodulin has been suggested earlier (Medvedeva et al. 1997).

We explored the effect of calmodulin binding on the time course of PAK phosphorylation of CaD22AA that has the two major sites blocked. Phosphorylation of the minor sites was significantly slower in the presence of Ca^{2+}-calmodulin than in the absence of Ca^{2+}-calmodulin. This indicates that Ca^{2+}-calmodulin binding to caldesmon impedes PAK access to the minor sites.

Foster et al. (2000) found that PAK phosphorylation of intact caldesmon attenuated the inhibition of actin-S1 ATPase. We observed attenuation of the inhibitory activity of CaD22 only under conditions where PAK phosphorylated the minor sites of CaD22. The phosphomimetic mutant of the major sites, CaD22DD, had the same inhibitory activity as CaD22 and CaD22AA. Furthermore, introducing negative charges at sites 672 and 702 had no effect on the inhibitory activity of the larger caldesmon construct, CaD35.

Prolonged incubation of CaD22WT, CaD22DD and CaD22AA with PAK did attenuate their inhibitory activities and all to the same extent. That is, phosphorylation of the minor sites of our construct was necessary for reversal of inhibitory activity irrespective of the state of residues 672 and 702.

Our results differ from those of Eppinga et al. (2006) who found complete reversal of inhibitory activity when the major PAK sites were mutated to glutamate residues. They reported that the phosphomimetic CaD39-PAKE had no inhibitory activity toward HMM ATPase at all. We do not know the reason for our different observations. It is clear though that phosphorylation of the minor sites does reduce the inhibitory activity of caldesmon.

PAK phosphorylation leads to a direct reduction in inhibitory activity of caldesmon. PAK phosphorylation also indirectly increases inhibitory activity by weakening binding to Ca^{2+}-calmodulin. Fig. 21 shows that the net activity depends on the concentration of Ca^{2+}-calmodulin and the number of caldesmon sites that are phosphorylated. For all caldesmon species examined the acto-S1 ATPase rates increased with increasing calmodulin concentrations. The rates of ATP hydrolysis in the presence of CaD22DD (mimicking phosphorylation of the major sites) were lower than those of wild type at all calmodulin concentrations. Caldesmon that was phosphorylated at the minor and major sites had higher activity than wild type at low calmodulin concentrations but the difference was abolished at high calmodulin concentrations.

It is interesting that a caldesmon mutant defective in Ca^{2+}-calmodulin binding sites fails to be recruited to podosomes, and fails to suppress the podosome formation. Selective control of caldesmon phosphorylation may

produce similar changes in calmodulin binding and produce similar cellular effects.

The results presented in this chapter suggest that the two main regulators of caldesmon in the cell, Ca^{2+}-calmodulin and phosphorylation, are not redundant mechanisms that substitute for one another. PAK phosphorylation and calmodulin cause different structural effects and allow smooth muscle contractility to be fine-tuned to the immediate needs of the cell.

Phosphorylation of the minor sites of caldesmon by PAK was very slow. It is possible that binding to some target molecule can alter the ability of the minor caldesmon sites to become phosphorylated. Molecular crowding in vivo may drastically change binding affinities of natively unfolded proteins; hence PAK might be more efficient in crowded environment (Yarmola et al, 2010). It is also possible that another kinase is able to rapidly phosphorylate the minor sites of caldesmon. To facilitate identification of possible kinases we identified the minor PAK phosphorylation sites of caldesmon. Those sites were Thr627, Ser631, Ser635 and Ser642. The location of those sites within CaD22 is shown in Fig. 22. Semi-quantitative analysis of the extracted ion chromatograms showed that Thr627 and Ser631 carried the greatest amounts of phosphate, while Ser642 had the least amount of phosphate. All 4 sites are clustered together, and the 3 most highly phosphorylated residues are located within the tropomyosin-binding region (residues 524-577and 579-635 (Wang et al. 1991)). Despite this location the attenuation of caldesmon inhibition did not require tropomyosin. Phosphorylation at the minor sites reduced the inhibitory activity of caldesmon in the absence of tropomyosin but to a lesser extent (data not shown).

If phosphorylation of the minor PAK sites (Thr627, Ser631, Ser635 or Ser642) serve a physiological role they are likely to be phosphorylated more rapidly than observed here. These sites could be better substrates for other kinases or phosphorylation may be linked to binding of caldesmon to a particular ligand.

Interestingly, one of the most heavily phosphorylated minor sites, Thr627, is adjacent to a myosin light chain kinase (MLCK) site, Thr626 (unpublished data from another lab). We investigated the properties of the triple phospho-mimicking mutant in which the major sites and one of the minor sites, Thr627, were mutated to Asp. We found that Thr627 by itself was unable to reproduce the effect of phosphorylation on all four minor sites, i.e. the triple mutant was unable to further reduce the binding affinity to Ca^{2+}-calmodulin and disinhibit the actin-activated S1-ATPase. That suggests that MLCK and Thr627 cannot be the kinase and the phosphorylation site that conveys the observed functional effects in the cell.

Another candidate is Ser635 that is a known substrate for Ca-Calmodulin kinase II (Ikebe and Reardon, 1990). The additive effects seen here may be an indication that caldesmon is coordinately regulated at several levels.

SUMMARY AND UNANSWERED QUESTIONS

Smooth muscle contraction may be altered through regulation of actin by actin-binding proteins. Interestingly, many actin-binding proteins contain long regions of intrinsic disorder (Permyakov et al. 2003; Czisch et al. 1993; Kim et al. 2000). It is not entirely clear yet how the disordered regions contribute to the regulation of actin. We wished to determine whether altering the unfolded regions of actin-binding proteins by a ligand binding or phosphorylation modifies their structures and functions.

First part of this project demonstrates that yet another actin-binding protein, fesselin, is natively unfolded. This information can be used as a guide for understanding the function of fesselin.

Fesselin is localized in dense bodies that are equivalent to Z-lines of skeletal muscle, where the ends of thin filaments from the adjacent sarcomeres overlap. Fesselin, as a natively unfolded protein, has many binding partners. Hence we speculate that fesselin works by organizing myofilaments into an ordered structure. It would be interesting to test this hypothesis in the cell by observing the effect of fesselin knockdown on the structural integrity of dense bodies in the cell.

Natively unfolded proteins are often involved in signaling and transcriptional regulation. Fesselin is a natively unfolded protein that shuttles between the nucleus and the Z-disks of myocytes depending on its differentiation stage and stress conditions, such as an increase in mechanical load (Weins et al, 2001). Hence fesselin might be involved in signal transduction leading to changes in gene expression between the dense bodies and the nucleus. Nuclear translocation of fesselin is regulated by phosphorylation (Faul et al. 2007). It would be interesting to check for changes in phosphorylation of fesselin upon increased force

applied to a smooth muscle. Uncovering such regulatory mechanism could potentially lead to a means of maintaining a healthy muscle tone.

Second part of this work demonstrated that another major actin-binding natively unfolded protein caldesmon that shares many properties with fesselin is regulated by Ca^{2+}-calmodulin and phosphorylation by PAK kinase through different mechanisms. We discovered a novel regulatory region between the residues 627-642 in the unfolded caldesmon C-terminus. Phosphorylation of this region alters both the ability of caldesmon to inhibit actomyosin ATPase and the interactions between caldesmon and Ca^{2+}-calmodulin. We identified four minor residues slowly phosphorylated by PAK. One of the still to be answered questions is which of the minor phosphorylation sites is responsible for the observed functional effects. Another unanswered question is whether or not this region is phosphorylated *in vivo.*

PAK kinase is slow to phosphorylate this region *in vitro*, but if the conformation of caldesmon is altered *in vivo* by binding to a target molecule or by molecular crowding, PAK might be more efficient in the cell. Alternatively, this region may be rapidly phosphorylated by a kinase other than PAK. Further research is needed to identify the kinase that phosphorylates the region between the residues 627-642, if indeed it could be phosphorylated in the cell.

The second part of the project also demonstrated that different combinations of phosphorylation state of the region between residues 627-642 of caldesmon, phosphorylation state of the major PAK sites (Ser 672 and Ser 702) and concentration of free calmodulin and free Ca^{2+} allow cells to “choose” between the regulatory modes with either high or low ATPase activity that can or cannot be altered by Ca^{2+}-calmodulin binding.

We demonstrated that the regulation of caldesmon is fairly complicated. Multiple kinases have been shown to phosphorylate caldesmon. Researchers have been focusing so far on the effects of one or another kinase on caldesmon function, and there has been an extensive discussion about which kinase is the most important in the regulation of caldesmon (Gorenne et al. 2004; Redwood et al. 1993; Childs et al. 1992). This work suggests that the signaling by several kinases might converge on caldesmon. Hence an approach is needed to look for global effects of caldesmon phosphorylation.

CHAPTER IV: MATERIALS AND METHODS

Protein preparation

Actin and myosin were isolated from rabbit back muscle (Spudich and Watt, 1971, Kielley and Harrington, 1960). Myosin subfragment 1 was made by digestion of myosin with chymotrypsin, for 10 minutes at 25^0C. The digestion product subfragment 1 (S1) retains the ability to bind to actin and hydrolyze ATP. (Weeds and Taylor, 1975).

Recombinant *(Arabidopsis)* calmodulin (pRZ72; a gift from Dr. Ralf Zielinski, University of Illinois at Urbana-Champaign, Urbana, IL, U.S.A.) was expressed in Escherichia coli BL21 cells and prepared as described by (Pedgio and Shea 1995). Smooth muscle tropomyosin was isolated from turkey gizzards (Bretcher 1984).

Fesselin was purified from turkey gizzards using the method of Leinweber et al. (1999). The 22 kDa C-terminal fragment of caldesmon, the 35 kDa C-terminal fragment of caldesmon, double alanine and double aspartic acid mutants were expressed in *Escherichia coli* and purified according to Fredricksen et al. (2003). p^{21}-activated kinase (GST-mPAK3, a gift from Dr. Alan Mak, Queen's University, Kingston, ON. U.S.A) was expressed in Escherichia coli BL21 cells and prepared as described before (Van Eyk et al. 1998).

The concentrations of the different CaD22 fragments and fesselin were determined by the Lowry assay with bovine serum albumin as a standard. The concentrations of other proteins were determined by absorbance at 280 nm, corrected for scattering at 340 nm, using the following extinction coefficients $E_{280}^{0.1\%}$: actin, 1.15, smooth muscle tropomyosin, 0.22, myosin S1, 0.75, and calmodulin, 0.19. The molecular masses assumed for the key proteins were myosin S1, 120000 Da, actin,

42000 Da, smooth muscle tropomyosin, 68000 Da, CaD22, 22000 Da, calmodulin, 16800 Da.

Stokes Radius Determination

Fesselin, Caldesmon 22, S1 and a series of known globular proteins were chromatographed on two Bio-Sil TSK-400 columns (80 x 7.8 nm and 600 x 7.5 mm) in tandem in a buffer containing 20 mM MOPS, pH 7.0, 0.2 M NaCl, 2 mM EGTA on a Waters 600E HPLC. Peak absorbances were monitored with a Waters 441 UV detector at 254 nm. The molecular weight of each substance was determined by laser light scattering on a Wyatt mini Dawn device with a Wyatt Optilab Rex refractive index detector. Calibration standards included thyroglobulin (R_s = 8.5 nm), alcohol dehydrogenase (R_s = 4.6 nm), bovine γ-globulin (R_s = 4.81 nm), myosin S1 (R_s = 4.8 nm, indicated by the arrow), chicken ovalbumin (R_s = 3.05 nm), carbonic anhydrase (R_s = 2.4 nm), equine myoglobin (R_s = 2.07 nm) and cytochrome C (R_s = 1.64 nm). The elution volume of proteins of known Stokes radius was used to determine the Stokes radius of fesselin, Cad22 and S1.

The relationship between the Stokes radius and the logarithm of molecular weight is given by the following equation:

$$\log(R_s) = a + b*\log(M), \qquad \text{(Equation 1)}$$

where a and b are the constants depending on the conformational state of a given protein (native, molten globule, premolten globule, natively unfolded coil, etc.) (Uversky 2002a).

Fluorescence measurements

The exposure of tryptophan residues to the solution and Ca^{2+}-calmodulin binding ware determined by changes in intrinsic tryptophan fluorescence of fesselin and CaD22. Fluorescence measurements were made on an Aminco Bowman II Luminescence Spectrometer (Thermo Electron Corp., Madison WI USA) having the cell compartment maintained at 20^{o}C with a circulating bath, in a buffer containing 10 mM MOPS pH 7.2, 100 mM NaCl, 1 mM dithiothreitol, 2 mM $CaCl_2$. Tryptophan fluorescence was measured with excitation and emission monochomators set to 295 nm and 340 nm, respectively. The absorbance of the protein solutions at the excitation wavelength was always kept low, so that inner filter effects could be neglected. Titrations with quenchers were done by adding small volumes of 5.6 M acrylamide. 10 minutes were allowed to pass before each measurement. The total dilution of the sample over the course of the titration was less than 10%. Spectra were corrected for the fluorescence contribution from calmodulin in the same buffer solution and for wavelength dependent lamp output. Because calmodulin lacks tryptophan residues, the correction for calmodulin was less than 5%.

Fluorescence quenching studies were analyzed using the Stern-Volmer equation for dynamic and static quenching:

$$F_0/F = 1 + (K_D + K_S)*[Q] + K_D*K_S*[Q]^2 \quad \text{(Equation 2)}$$

where F_0 and F are the fluorescence intensities in the absence and presence of quencher, respectively; K_D and K_S are the dynamic and static Stern-Volmer quenching constants, Q is the concentration of the quencher.

Calmodulin binding data were analyzed using SigmaPlot 11.2 software (Systat Software, INC. San Jose CA, USA). The multiple sets of binding data were fitted to a rectangular hyperbola and the K_d values were extracted:

$Y = (B_{max}*X)/(K_d + X)$ (Equation 3)

where B_{max} is a number of binding sites; Kd is an equilibrium dissociation constant.

The 95% confidence intervals (the region of uncertainties in the predicted values over a range of values for the independent variable) were also estimated using SigmaPlot 11.2.

Circular Dichroism

Circular dichroism spectra were obtained with JASKO J-810 spectrometer. Spectra were recorded using 0.01-cm pathlength cell at room temperature (pH titration experiment) in a buffer containing 50 mM potassium chloride and 2 mM sodium phosphate. Spectra of appropriate buffers were recorded and subtracted from the protein spectra. For all spectra, the average of 8 scans was obtained. The reliability of the data was monitored by recording high tension voltage. The difference between absorbance of left circularly polarized and right circularly polarized light (ΔA) was measured, and mean residue ellipticity (M.R.E.) was calculated as described below:

$M.R.E = 3298.2*\Delta A/(C*l*n)$ (Equation 4)

Where C is the molar concentration, l is the path length in centimeters, n is the number of residues in the protein.

Primary Structure Analysis of fesselin

Sequence information was obtained from GenBank ABU55374.1 for fesselin from turkey meleagris gallopavo (Schroeter et al. 2008). Sequence information was analyzed using the PONDR (Predictor of Natural Disordered Regions) program and Network Protein Sequence Analysis web server. (Combet et al. 2000).

Phosphorylation of Caldesmon

CaD22 (generally 1 mg/ml) was phosphorylated by constitutively active GST-mPAK3 (~10 µg/µl). All the phosphorylation reactions were carried out at 25^0C for indicated time, in 20 mM Tris pH 7.5, 100 mM NaCl, 5 mM $MgCl_2$, 0.5 mM dithiothreitol. The reactions were initiated by addition of 1 mM ATP. Phosphorylated protein was used for experimental purposes immediately. Phosphorylation times are given in the text.

Detection of phosphorylation

The extent of phosphorylation was determined by Non-equilibrium isoelectric focusing gel electrophoresis (NEIEF) as described by Kobayashi et al (2005). Gels contained 8 M urea, 5% acrylamide, 0.8% ampholyte pH 3.0-10.0 and 1.2% ampholyte pH 8.0-10.0 (BioRad, CA). Sample loading buffer contained 8 M urea, 10mM EDTA and 1% ampholyte pH 3.0-10.0. The running times were 30 minutes at 100 V, 40 minutes at 200 V and 20 minutes at 500 V. The gels were soaked in fixing solution containing 10% methanol and 5% acetic acid, and then stained with Coomassie Blue stain.

Phosphorylation time course measurements

Time courses of phosphorylation were determined by measuring the incorporation of ^{32}P into caldesmon fragments at various time intervals with a filter paper assay (Conti and Adelstein, 1991). Caldesmon fragments were phosphorylated by PAK at 25°C in 20 mM Tris-HCl pH 7.5, 100 mM NaCl, 5 mM $MgCl_2$, 1 mM dithiothreitol and 1 mM ^{32}P-ATP ($4*10^5$ cpm/nmol). Aliquots were drawn at different times after initiation of phosphorylation and placed onto Whatman grade 3 filter circles (2.3 cm diameter). Filters were dropped immediately into ice-cold 10% TCA, 8% sodium pyrophosphate (w/v), followed by 3 subsequent washes for 10-15 minutes with 10% TCA, 2% sodium pyrophosphate at room temperature. The filters were then washed in 95% ethanol and finally in acetone. The ^{32}P activity of the filters was determined by liquid scintillation counting.

Identification of the phosphorylation sites

The sites of phosphorylation were identified by mass spectrometry. The CaD22 protein bands were excised from SDS gels, reduced, alkylated and digested with modified trypsin (Promega). The peptides were analyzed by LC-MS/MS using capillary HPLC with a 75 μm nanocolumn and a Thermo Electron LTQ quadrapole ion trap mass spectrometer. The resulting masses and spectra were searched against a database using TurboSequest (Chittum et al. 1998; Eng et al. 1994) with the Proteomics Browser interface (William Lane, Harvard Microchemistry and Proteomics Analysis Facility). Extracted Ion Chromatograms of full MS scan were performed on the m/z values that match the phosphorylated peptides and corresponding non-phosphorylated peptides using a mass error window of

±5ppm. The peptide identities of integrated peaks were verified based on retention times of the MS/MS spectra. Mass Spectral analysis was performed at the Wistar proteomics facility, Philadelphia, PA.

ATPase Rate measurements

Rates were determined by measuring the time dependence of $^{32}P_i$ formation from γ^{32}P-labeled ATP at 25ºC. Concentrations of actin, smooth muscle tropomyosin and myosin S1 were 10 μM, 2.2 μM and 0.1 μM, respectively. The final solution composition was 1 mM ATP, 3 mM $MgCl_2$, 31 mM NaCl, 10 mM imidazole pH 7.0. The reaction volume was 1 ml. Aliquots of 0.2 ml were removed at different time points and quantified as described earlier (Chalovich and Eisenberg, 1982). A minimum of 4 time points were taken over the 10-15 minute period to establish the rate. The measured rates are the initial rates since the production of ^{32}P was linear over this time period.

REFERENCES

ADAM, L.P. and HATHAWAY, D.R. 1993. IDENTIFICATION OF MITOGEN-ACTIVATED PROTEIN KINASE PHOSPHORYLATION SEQUENCES IN MAMMALIAN H-Caldesmon. FEBS Lett. 322, 56-60.

ADESTEIN, R.S. and SELLERS, J.R. 1987. Effects of calcium on vascular smooth muscle contraction. Am. J. Cardiol. 59, 4B-10B.

ADLER, A.J., GREENFIELD, N.J., and FASMAN, G.D. 1973. Circular dichroism and optical rotatory dispersion of proteins and polypeptides. Methods Enzymol. 27, 675-735.

ALAHYAN, M., WEBB, M.A., MARSTON, S.B. and EL-MEZGUELDI, M. 2006. The mechanism of smooth muscle caldesmon-tropomyosin inhibition of the elementary steps of the actomyosin ATPase. J. Biol. Chem. 281, 19433-19448.

AYED, A., MULDER, F.A., YI, G.S., LU, Y., KAY, L.E. and ARROWSMITH, C.H. 2001. Latent and active p53 are identical in conformation. Nature Struct. Biol. 8, 756-760.

BALAZS, A., CSIZMOK, V., BUDAY, L., LASZLO, R., KISS, M., BOKOR, R., UDUPA, M., TOMPA, K. and TOMPA, P. 2009. High levels of structural disorder in scaffold proteins as exemplified by a novel neuronal protein, Caskin1. FEBS J. 276, 3744-3756.

BANNISTER, A.J. and KOUZARIDES, T. 1995. CBP-induced stimulation of c-Fos activity is abrogated by E1A. EMBO J. 14, 4758-4762.

BEALL, B.B., and CHALOVICH, J.M. 2001. Fesselin, a synaptopodin-like protein, stimulates actin nucleation and polymerization. Biochemistry, 40, 14252-14259.

BELL, S., KLEIN, S., MULLER, L., HANSEN, S. and BUCHNER, J. 2002. p53 contains large unstructured regions in its native state. J. Mol. Biol. 322, 917-927.

BLASIUS, T.L., CAI, D., JIH, G.T., TORET, C.P. and VERHEY, K.J. 2007. Two binding partners cooperate to activate the molecular motor Kinesin-1. J. Cell Biol. 176, 11 - 17.

BLUMENSCHEIN, T., STONE, D.B., FLETTERICK, R.J., MENDELSON, R.A. and Sykes, B.D. 2006. Dynamics of the C-terminal region of TnI in the troponin complex in solution. Biophys. J. 90, 2436-2444.

BOURHUS, J-M., JOHANSSON, K., RECEVEUR-BRECHOT, V., OLDFIELD, C.J., DUNKER, K.A., CANARD, B. and LONGHI, S. 2004. The C-terminal domain of measles virus nucleoprotein belongs to the class of intrinsically disordered proteins that fold upon binding to their physiological partner. Virus Res. 99, 157-167.

BRETSCHER, A. 1984. Smooth muscle caldesmon. Rapid purification and F-actin cross-linking properties. J. Biol. Chem. 259, 12873-12880.

BRYAN, J. 1989. Caldesmon, acidic amino acids and molecular weight determinations. J. Muscle Res. Cell Motil. 10, 95-96.

BRYAN, J. and LEE, R. 1991. Sequence of an avian non-muscle caldesmon. J. Muscle Res. Cell Motil. 12, 372-375.

CAMPBELL, K.K., TERRELL, A.R., LAYBOURN, P.J. and LUMB, K.J. 2000. Intrinsic structural disorder of the C-terminal activation domain from the bZIP transcription factor Fos. Biochemistry 39, 2708-2713.

CHALOVICH, J.M. and EISENBERG, E. 1982. Inhibition of actomyosin ATPase activity by troponin-tropomyosin without blocking the binding of myosin to actin. J Biol Chem. 257, 2432-2437.

CHALOVICH, J.M., SEN, A., RESETAR, A., LEINWEBER, B., FREDRICKSEN, R.S., LU, F., and CHEN, Y-D. 1998. Caldesmon: binding to actin and myosin and effects on elementary steps in the ATPase cycle. Acta Physiol. Scand. 164, 427-435.

CHALOVICH, J.M., HEMRIC, M.E. and VELAZ, L. 1990. Regulation of ATP hydrolysis by caldesmon. A novel change in the interaction of myosin with actin. Ann. N.Y. Acad. Sci. 599, 85-89.

CHILDS, T.J., WATSON, M.H., SANGHERA, J.S., CAMPBELL, D.L., PELECH, S.L., and MAK, A.S. 1992. Phosphorylation of smooth muscle caldesmon by mitogen-activated protein (MAP) kinase and expression of MAP kinase in differentiated smooth muscle cells. J. Biol. Chem. 267, 22853-22859.

CHITTUM, H.S., LANE, W.S., CARLSON, B.A., ROLLER, P.P., LUNG, F.D., LEE, B.J. and HATFIELD, D.L. 1998. Rabbit beta-globin is extended beyond its UGA stop codon by multiple suppressions and translational reading gaps. Biochemistry 37, 10866-10870.

COEYTAUX, K. and POUPON, A. 2005. Prediction of unfolded segments in a protein sequence based on amino acid composition. Bioinformatics 21, 1891-1900.

COMBET, C., BLANCHET, C., GEOURJON, C., and DELEAGE, G. 2000. NPS@: Network Protein Sequence Analysis. Trends Biochem. Sci. 25, 147-150.

CONTI, M.A., and ADELSTEIN, R.S. 1981. The relationship between calmodulin binding and phosphorylation of smooth muscle myosin kinase by the catalytic subunit of 3':5' cAMP- dependent protein kinase. J. Biol. Chem. 256, 3178-3181.

CZISCH, M., SCHLEICHER, M., HORGER, S., VOELTER, W. and HOLAK, T.A. 1993. Conformation of thymosin beta 4 in water determined by NMR spectroscopy. Eur. J. Biochem. 218, 335-344.

D'ANGELO, G., GRACEFFA, P., WANG, C.A., WRANGLE, J. and ADAM, L.P. 1999. Mammal-specific, ERK-dependent, caldesmon phosphorylation in smooth muscle. Quantitation using novel anti-phosphopeptide antibodies. J. Biol. Chem. 274, 30115-30121.

DABROWSKA, R., HINSSEN, H., GALAZKIEWICZ, B., and NOWAK, E. 1996. Modulation of gelsolin-induced actin-filament severing by caldesmon and tropomyosin and the effect of these proteins on the actin activation of myosin Mg(2+)-ATPase activity. Biochem. J. 315, 753-759.

DELLER, T., KORTE, M., CHABANIS, S., DRAKEW, A., SCHWEGLER, H., STEFANI, J.G., ZUNIGA, A., SCHWARZ, K., BONHOEFFER, T., ZELLER, R., FROTSCHER, M. and MUNDEL, P. 2003. Synaptopodin-

deficient mice lack a spine apparatus and show deficits in synaptic plasticity. Proc. Natl. Acad. Sci. U.S.A. 100, 10494-10499.

DHARMAWARDHANE, S., SANDERS, L.C., MARTIN, S.S., DANIELS, R.H. and BOKOCH, G.M. 1997. Localization of p^{21}-activated kinase 1 (PAK1) to pinocytic vesicles and cortical actin structures in stimulated cells. J. Cell Biol. 138, 1265-1278.

DUNKER A.K., OBRADOVIC, Z., ROMERO, P., GARNER, E.C. and BROWN, C.J. 2000. Intrinsic protein disorder in complete genomes. Genome Informatics Series: Proceedings of the Workshop on Genome Informatics. 11, 161–171.

DUNKER, A.K., BROWN, C.J., LAWSON, J.D., IAKOUCHEVA, L.M. and OBRADOVIC, Z. 2002. Intrinsic disorder and protein function. Biochemistry 41, 6573-6582.

DUNKER, K., CORTESE, M.S., ROMERO, P., IAKOUCHEVA, L.M. and UVERSKY, V.N. 2005. Flexible nets. The role of intrinsic disorder in protein interaction nerworks. FEBS 272, 5129.

ENG, J.K., MCCORMICK, L. and YATES, J.R.III. 1994. An approach to correlate tandem mass spectral data of peptides with amino acid sequences in a protein database. J.Am. Soc. Mass. Spectrom. 5, 976−989.

EPPINGA, R.D., LI, Y., LIN, J.L., MAK, A.S. and LIN, J.J. 2006. Requirement of reversible caldesmon phosphorylation at p21-activated kinase-responsive sites for lamellipodia extensions during cell migration. Cell Motil. Cytoskeleton 63, 543-562.

EPSTEIN, N.D. and DAVIS, J.S. 2003. Sensing stretch is fundamental. Cell 112, 147-150.

FAY, F.S., FUJIWARA, K., REES, D.D. and FOGARTY, K.E. 1983. Distribution of alpha-actinin in single isolated smooth muscle cells. J. Cell Biol. 96, 783-795.

FOSTER, D.B., SHEN, L.H., KELLY, J., THIBAULT, P., VAN EYK, J.R. and MAK, A.S. 2000. Phosphorylation of caldesmon by p21-activated kinase. Implications for the Ca^{2+} sensitivity of smooth muscle contraction. J. Biol. Chem. 275, 1959-1965.

FREDRICKSEN, S., CAI, A., GAFUROV, B., RESETAR, A. and CHALOVICH, J.M. 2003. Influence of ionic strength, actin state, and caldesmon construct size on the number of actin monomers in a caldesmon binding site. Biochemistry 42, 6136-6148.

FUJII, T., IMAI, M., ROSENFELD, G.C. and BRYAN, J. 1987. Domain mapping of chicken gizzard caldesmon. J. Biol. Chem. 262, 2757-2763.

FUXREITER, M., SIMON, I., FRIEDRICH, P. and TOMPA, P. 2004. Preformed structural elements feature in partner recognition by intrinsically unstructured proteins. J. Mol. Biol. 338, 1015-1026.

FUXREITER, M., TOMPA, P. and SIMON, I. 2007. Local structural disorder imparts plasticity on linear motifs. Bioinformatics 23, 950-956.

GAO, Y., YE, L.H., KISHI, H., OKAGAKI, T., SAMIZO, K., NAKAMURA, A., and KOHAMA, K. 2001. Myosin light chain kinase as a multifunctional regulatory protein of smooth muscle contraction. IUBMB Life 51, 337–344.

GALAZKIEWICZ, B., MOSSAKOWSKA, M., OSINSKA, H. and DABROWSKA, R. 1985. Polymerization of G-actin by caldesmon. FEBS Lett. 184, 144-149.

GALAZKIEWICZ, B., BELAGYI, J., and DABROWSKA, R. 1989. The effect of caldesmon on assembly and dynamic properties of actin. FEBS 181, 607-614.

GALZITSKAYA, O.V., GARBUZYNSKIY, S.O. and LOBANOV, M.Y. 2006. Prediction of natively unfolded regions in protein chain. Mol. Biol. 40, 298-304.

GOLEY, E.D. and WELCH, M.D. 2006. The ARP2/3 complex: an actin nucleator comes of age. Nat. Rev. Mol. Cell Biol. 7, 713-726.

GORENNE, I., XIAOLING, S., and MORELAND, R.S. 2004. Caldesmon phosphorylation is catalyzed by two kinases in permeabilized and intact vascular smooth muscle. J. Cell Physiol. 198, 461-469.

GREENE, L.E., and EISENBERG, E. 1980**.** Cooperative Binding of Myosin Subfragment-1 to the Actin-Troponin-Tropomyosin Complex. PNAS 77, 2616-2620.

HACKNEY, D.D., LEVITT, J.D., and SUHAN, J. 1992. Kinesin undergoes a 9 S to 6 S conformational transition. J. Biol. Chem. 267, 8696 - 8701.

HASIMOTO, Y., and SODERLING, T.R. 1990. Phosphorylation of smooth muscle myosin light chain kinase by Ca^{2+}/calmodulin-dependent protein kinase II: comparative study of the phosphorylation sites. Arch Biochem Biophys. 278, 41-45.

HEMRIC, M.E. and CHALOVICH, J.M. 1988. Effect of caldesmon on the ATPase activity and the binding of smooth and skeletal myosin subfragments to actin. J. Biol. Chem. 263, 3055-3058.

HEUMANN, H.G. 1970. A regular actin filament lattice in a vertebrate smooth muscle. Experimentia 26, 1131-1132.

HODGKINSON, J.L., MARSTON, S.B., CRAIG, R., VIBERT, P., and LEHMAN, W. 1997. Three-dimensional image reconstruction of reconstituted smooth muscle thin filaments: effect of caldesmon. Biophys. J. 72, 2398-2404.

HUANG, R., LIANSHENG, L., GUO, H. and WANG, C-L. A. 2003. Caldesmon binding to actin is regulated by calmodulin and phosphorylation via different mechanisms. Biochemistry 42, 2513-2523.

IKEBE, M., INAGAKI, M., KANAMARU, K., and HIDAKA, H. 1985. Phosphorylation of smooth muscle myosin light chain kinase by Ca^{2+}-activated, phospholipid-dependent protein kinase. J. Biol. Chem. 260, 4547-4550.

IKEBE, M. and REARDON, S. 1988. Binding of caldesmon to smooth muscle myosin. J. Biol. Chem. 263, 3055-3058.

IKEBE, M. and REARDON, S. 1990. Phosphorylation of smooth muscle caldesmon by calmodulin-dependent protein kinase II. Identification of the phosphorylation sites. J. Biol. Chem. 265, 17607-17612.

JIANG, Q., HUANG, R., CAI, S. and WANG, C-L.A. 2010. Caldesmon regulates the motility of vascular smooth muscle cells by modulating the actin cytoskeleton stability. J. Biomed. Sci. 17, 6.

JING, L., LIU, L., YU, Y.P., DHIR, R., ACQUAFONDADA, M., LANDSITTEL, D., CIEPLY, K., WELLS, A. and LUO, J.H. 2004. Expression of Myopodin Induces Suppression of Tumor Growth and Metastasis. Am. J. Pathol. 164, 1799-1806.

KAMM, K.E. and STULL, J.T. 1985. The function of myosin and myosin light chain kinase phosphorylation in smooth muscle. Annu. Rev. Pharmacol. Toxicol. 25, 593.

KATAYAMA, E., SCOTT-WOO, G., and IKEBE, M. 1995. Effect of caldesmon on the assembly of the smooth muscle myosin. J. Biol. Chem. 270, 3919-3925.

KHAYMINA, S.S, KENNEY, J.M., SCHROETER, M.M., and CHALOVICH, J.M. 2007. Fesselin is a natively unfolded protein. J. Proteome Res. 6, 3648-3654.

KIELLEY, W.W. and W.F. HARRINGTON. 1960. A model for the myosin molecule. Biochim. Biophys. Acta 41, 401-421.

KIM, A.S., KAKALIS, L.T., ABDUL-MANAN, N., LIU, G.A. and ROSEN, M.K. 2000. Autoinhibition and activation mechanisms of the Wiskott-Aldrich syndrome protein. Nature 404, 151-158.

LAZARIDES, E. 1976. Actin. Alpha-actinin and tropomyosin interactions in the structural organization of actin filaments in nonmuscle cells. J. Cell Biol. 68, 202-219.

LEINWEBER, B.D., FREDRICKSEN, R.S., HOFFMAN, D.R. and CHALOVICH, J.M. 1999. Fesselin: a novel synaptopodin-like actin binding protein from muscle tissue. J. Muscle Res. Cell Motil. 20, 539-545.

LI, Y., JE, H-D., MALEK, S. and MORGAN, K.G. 2003. ERK1/2-mediated phosphorylation of myometrial caldesmon during pregnancy and labor. Am. J. Physiol. 284, R192-R199.

LINDING, R., RUSSEL, R.B., NEDUVA, V. and GIBSON, T.J. 2003. GlobProt: Exploring protein sequences for globularity and disorder. Nucleic Acids Res. 31, 3701-3708.

MARSTON, S.B. and REDWOOD, C.S. 1992. Inhibition of actin-tropomyosin activation of myosin MgATPase activity by the smooth muscle regulatory protein caldesmon. J. Biol. Chem. 268, 12317-12320.

MASATO, T., NUMATA, T., KATOH, T., MORITA, F., and YAZAWA, M. 1997. Crosslinking of telokin to chicken gizzard smooth muscle myosin. J. Biochem. 121, 225-30.

MEDVEDEVA, M.V., KOLOBOVA, E.A., HUBER, P.A., FRASER, I.D., MARSTON, S.B. and GUSEV, N.B. 1997. Mapping of contact sites in the caldesmon-calmodulin complex. Biochem J. 324, 255-262.

MOHAN, A., OLDFIELD, C.J., RADIVOJAC, P., VACIC, V., CORTESE, M.S., DUNKER, K.A. and UVERSKY, V.N. 2006. Analysis of Molecular Recognition Features (MoRFs). J. Mol. Biol. 362, 1043-1059.

MORITA, T., MAYANAGI, T., YOSHIO, T., and SOBUE, K. 2006. Changes in the balance between caldesmon regulated by p21-activated kinases and the Arp2/3 complex govern podosome formation. J. Biol. Chem. 282, 8454-8463.

MUNDEL, P., HEID, H.W., MUNDEL, T. M., KRUGER, M., REISER, J. and KRIZ, W. 1997. Synaptopodin: An Actin-associated Protein in Telencephalic Dendrites and Renal Podocytes. J. Cell Biol. 139, 193-204.

NGAI, P.K. and WALSH, M.P. 1984. Inhibition of smooth muscle actin-activated myosin Mg^{2+}-ATPase activity by caldesmon. J. Biol. Chem. 259, 13656-13659.

NGAI, P.K. and WALSH, M.P. 1987. The effects of phosphorylation of smooth muscle caldesmon. Biochem. J. 244, 417-425.

NISHIKAWA, M., SHIRAKAWA, S. and ADELSTEIN, R.S. 1985. Phosphorylation of smooth muscle myosin light chain kinase by protein

kinase C. Comparative study of the phosphorylated sites. J. Biol. Chem. 260, 8978-8983.

OLDFIELD, C.J., CHENG, Y., CORTESE, M.S., ROMERO, P., UVERSKY, V.N. and DUNKER, K.A. 2005. Coupled binding and folding with α-helix-forming Molecular Recognition Elements. Biochemistry 44, 12454-12470.

PEDGIO, S and M.A. SHEA. 1995. Quantitative endoproteinase GluC footprinting of cooperative Ca^{2+} binding to calmodulin: proteolytic susceptibility of E31 and E87 indicates interdomain interactions. Biochemistry 34, 1179-1196.

PERMYAKOV, S.E., MILLET, I.S., DONIACH, S., PERMYAKOV, E.A., and Uversky, V.N. 2003. Natively unfolded C-terminal domain of caldesmon remains substantially unstructured after the effective binding to calmodulin. Proteins 53, 855-862.

PHAM, M. and CHALOVICH, J.M. 2005. Smooth muscle alpha-actinin binds tightly to fesselin and attenuates its activity towards actin polymerization. J. Muscle Res. Cell Motil. 27, 45-51.

POLLARD, T.D., BLANCHOIN, L., and MULLINS, R.D. 2000. Molecular mechanisms controlling actin filament dynamics in nonmuscle cells. Annu. Rev. Bioph. Biom. 29, 545-576.

PRITCHARD, K. and MARSTON, S.B. 1989. Ca2+-calmodulin binding to caldesmon and the caldesmon-actin-tropomyosin complex. Its role in Ca2+ regulation of the activity of synthetic smooth-muscle thin filaments. Biochem. J. 257, 839-843.

PYLE, W.G. and SOLARO, R.J. 2004. At the crossroad of myocardial signaling: the role of Z-disks in intracellular signaling and cardiac function. Circ. Res. 94, 296-305.

RAO, J. and LI, N. 2004. Microfilament actin remodeling as a potential target for cancer drug development. Curr Cancer Drug Targets 4, 345-54.

REDWOOD, C.S., MARSTON, S.B., and GUSEV, N.B. 1993. The functional effects of mutations Thr673→Asp and Ser702→Asp at the Pro-

directed kinase phosphorylation sites in the C-terminus of chicken gizzard caldesmon. FEBS 327, 85-89.

RENEGAR, R.H., CHALOVICH, J.M., LEINWEBER, B.D., ZARY, J.T. and SCHROETER, M.M. 2009. Localization of the actin-binding protein fesselin in chicken smooth muscle. Histochem. Cell Biol. 131, 191-196.

ROMERO, P., OBRADOVIC, Z., LI, X., GARNER, E.E., BROWN, C.J. and DUNKER, A.K. 2001. Sequence complexity of disordered proteins. Proteins 42, 38-48.

SANCHEZ-CARBAYO, M., SCHWARZ, K., CHARYTONOWICZ, E., CORDON-CARDO, C. and MUNDEL, P. 2003. Tumor suppressor role for myopodin in bladder cancer: loss of nuclear expression of myopodin is cell-cycle dependent and predicts clinical outcome. Oncogene 22, 5298-5305.

SELLERS, J.R., and KNIGHT, P.J. 2007. Folding and regulation in myosins II and V. J. Muscle Res. Cell M. 28, 363-370.

SCHROETER, M. and CHALOVICH, J.M. 2004. Ca^{2+}-calmodulin regulates fesselin-induced actin polymerization. Biochemistry 43, 13875-13882.

SCHROETER, M.M. and CHALOVICH, J.M. 2005. Fesselin binds to actin and myosin and inhibits actin-activated ATPase activity. J. Muscle Res. Cell M. 26, 183-189.

SCHROETER, M.M., BEALL, B., HEID, H.W. and CHALOVICH, J.M. 2008. The actin binding protein, fesselin, is a member of the synaptopodin family. Biochem. Bioph. Res. Co. 371, 582-586.

SICKMEIER, M., HAMILTON, J.A., LEGALL, T., VACIC, V., CORTESE, M.S., TANTOS, B.S., TOMPA, P., CHEN, J., UVERSKY, V.N., OBRADOVIC, Z. and DUNKER, K.A. 2007. DisProt: the Database of Disordered Proteins. Nucleic Acids Res. 35, D786–D793.

SOBUE, K., MURAMOTO, Y., FUJITA, M., and KAKIUCHI, S. 1981. Purification of a calmodulin-binding protein from chicken gizzard that interacts with F-actin. Proc. Natl. Acad. Sci. USA 78, 5652-5655.

SPUDICH, J. A. and WATT, S. 1971. The regulation of rabbit skeletal muscle contraction. I. Biochemical studies of the interaction of the tropomyosin–troponin complex with actin and the proteolytic fragments of myosin. J. Biol. Chem. 246, 4866–4871.

STOCK, M.F., GUERRERO, J., COBB, B., EGGERS, C.T., HUANG, T-G., Li, X., and HACKNEY, D.D. 1999. Formation of the Compact Confomer of Kinesin Requires a COOH-terminal Heavy Chain Domain and Inhibits Microtubule-stimulated ATPase Activity. J. Biol. Chem. 274, 14617.

SUTHERLAND, C., and WALSH, M.P. 1989. Phosphorylation of caldesmon prevents its interaction with smooth muscle myosin. J. Biol. Chem. 264, 578-583.

SZPACENKO, A., WAGNER, G., DABROWSKA, R. and Ruegg, J.C. 1985. Caldesmon-induced inhibition of the ATPase activity of actomyosin and contraction of skinned fibers of chicken gizzard smooth muscle. FEBS 192, 9-12.

SZPACENKO, A. and DABROWSKA, R. 1986. Functional domain of caldesmon. FEBS Lett. 202, 182-186.

TANI, E. 2002. Molecular mechanisms involved in development of cerebral vasospasm. Neurosurg Focus 12(3).

TCHERKASSKAYA, O. and UVERSKY, V.N. 2001. Denatured collapsed states in protein folding:example of apomyoglobin. Protein 44, 244-254.

TOMPA, P. 2002. Intrinsically unstructured proteins. Trends Biochem. Sci. 27, 527-533.

TOMPA, P., SZASZ, C. and BUDAY, L. 2005. Structural disorder throws new light on moonlighting. Trends Biochem Sci. 30, 484–489.

UEHARA, Y., CAMPBELL, G.R., BURNSTOCK, G. 1971. Cytoplasmic filaments in developing and adult vertebrate smooth muscle. J. Cell Biol. 50, 484-497.

UVERSKY, V.N., GILLESPIE, J.R. and FINK, A.L. 2000. Why are “natively unfolded” proteins unstructured under physiologic conditions. Proteins 41, 415-427.

UVERSKY, V. N. 2002a. What does it mean to be Natively Unfolded? Eur. J. Biochem. 269, 2-12.

UVERSKY, V.N. 2002b. Natively unfolded proteins: a point where biology waits for physics. Protein Sci. 11, 739-756.

VAN EYK, J.E., ARRELL, D.K., FOSTER, D.B., STRAUSS, J.D., HEINONEN, T.Y., FURMANIAK-KAZMIERCZAK, E., COTE, G.P. and MAK, A.S. 1998. Different molecular mechanisms for Rho family GTPase-dependent, Ca^{2+}-independent contraction of smooth muscle. J. Biol. Chem. 273, 23433-23439.

VELAZ, L., HEMRIC, M.E., BENSON, C.E. and CHALOVICH, J.M. 1989. The binding of caldesmon to actin and its effects on the ATPase activity of soluble myosin subfragments in the presence and absence of tropomyosin. J. Biol. Chem. 264, 9602-9610.

VOROTNIKOV, A.V., GUSEV, N.B., HUA, S., COLLINS, J.H., REDWOOD, C.S. and MARSTON, S.B. 1994. Phosphorylation of aorta caldesmon by endogenous proteolytic fragments of protein kinase C. J. Muscle Res. Cell Motil. 15, 37-48.

WANG, C-L.A., WANG, L-W.C., XU, S.A., LU, R.C., SAAVEDRA-ALANIS, V., and BRYAN, J. 1991. Localization of the calmodulin- and the actin-binding sites of caldesmon. J. Biol. Chem. 266, 9166-9172.

WARD, J.J., SODHI, J.S., MCGUFFIN, L.J., BUXTON, B.F. and JONES, D.T. 2004. Prediction and functional analysis of native disorder in proteins from the three kingdoms of life. J. Mol. Biol. 337, 635-645.

WEEDS, A.G. and TAYLOR, R.S. 1975. Separation of subfragment-1 isozymes from rabbit skeletal muscle myosin. Nature 257, 54–56.

WEINS, A., SCHWARZ, K., FAUL, C., BARISONI, L., LINKE, W.A. and MUNDEL, P. 2001. Differentiation- and stress-dependent nuclear cytoplasmic redistribution of myopodin, a novel actin-bundling protein. J. Cell Biol. 155, 393-404.

WRIGHT, P.E. and DYSON, H.J. 1999. Intrinsically unstructured proteins: re-assessing the protein structure-function paradigm. J. Mol. Biol. 293, 321-331.

XIE, H., VUCETIC, S., IAKOUCHEVA, L.M., OLDFIELD, C.J., DUNKER, K.A., UVERSKY, V.N. and OBRADOVIC, Z. 2007a. Functional anthology of intrinsic disorder. 1. Biological processes and functions of proteins with long disordered regions. J. Proteome Res. 6, 1882-1898.

XIE, H., VUCETIC, S., IAKOUCHEVA, L., OLDFIELD, C., DUNKER, K., OBRADOVIC, Z. and UVERSKY, V. 2007b. Functional anthology of intrinsic disorder. 3. Ligands, post-translational modifications, and diseases associated with intrinsically disordered proteins. J. Proteome Res. 6, 1917.

XU, C., CRAIG, R., TOBACMAN, L., HOROWITZ, R., and LEHMAN, W. 1999. Tropomyosin positions in regulated thin filaments revealed by cryoelectron microscopy. Biophys. J. 77, 985-992.

XU, W., DOSHI, A., LEI, M., ECK, M.J. and HARRISON, S.C. 1999b. Crystal structures of c-Src reveal features of its autoinhibitory mechanism. Mol. Cell 3, 629-638.

YAMAGUCHI, H., LORENZ, M., KEMPIAK, S., SARMIENTO, C., CONIGLIO, S., SYMONS, M., SEGALL, J., EDDY, R., MIKI, H., TAKENAWA, T., and CONDEELIS, J. 2005. Molecular mechanisms of invadopodium formation: the role of the N-WASP-Arp2/3 complex pathway and cofilin. J. Cell Biol. 168, 441-452.

YAMAKITA, Y., YAMASHIRO, S. and MATSUMURA, F. 1992. Characterization of mitotically phosphorylated caldesmon. J. Biol. Chem. 267, 12022-12029.

YAMASHIRO, S., YAMAKITA, Y., HOSOYA, H. and MATSUMURA, F. 1991. Phosphorylation of non-muscle caldesmon by p34cdc2 kinase during mitosis. Nature 349, 169-172.

YARMOLA, E.G., TAUS, P., KORYTOV, D. and BUBBS, M. 2010. Effects of molecular cowding in actin polymerization. Biophys. J. 98, 154a.

ZHANG, Y., FENG, X.H. and DERYNCK, R. 1998. Smad3 and Smad4 cooperate with c-Jun/c-Fos to mediate TGF-beta-induced transcription. Nature 394, 909-913.

ZHOU, N., YUAN, T., MAK, A.S., VOGEL, H.J. 1997. NMR studies of caldesmon-calmodulin interactions. Biochemistry 36, 2817-2825.

ZOR, T.B., MAYR, M., DYSON, H.J., MONTMINY, M.R. and WRIGHT, P.E. 2002. Roles of phosphorylation and helix propensity in the binding of the KIX domain of CREB-binding protein by constitutive (c-Myb) and inductive (CREB) activators. J. Biol. Chem. 277, 42241-42248.

APPENDIX I. AN ATTEMPT TO EXPRESS A 10 KD FRAGMENT OF FESSELIN

Identification of Ca^{2+}-Calmodulin binding site in the sequence of fesselin

For our analysis we used the sequence of fesselin from turkey meleagris gallopavo {GenBank: ABU55374.1} (Schroeter et al. 2008).

It is possible that fesselin contains several calmodulin-binding sites. In fact, a number of data produced in our lab could not be explained by the assumption that fesselin binds only 1 calmodulin molecule (Schroeter and Chalovich, 2004).

To determine where the possible calmodulin-binding sites may be, the sequence of fesselin was submitted to the program “Calmodulin target database”. This program compares a submitted sequence to the known calmodulin-binding sequences and also analyzes the sequence for possible binding sites based on the evaluation criteria, such as hydropathy, alpha-helical propensity, residue weight, residue charge, hydrophobic residue content, helical class and occurrence of particular residues. As an output, the program gives each amino acid in the sequence a score. The higher is the score of a particular stretch of amino acids, the greater is the probability of this stretch to bind Ca^{2+}-calmodulin. Zero scores indicate the unlikely involvement in the formation of a calmodulin-binding site.

No matches to the sequences known to bind calmodulin were found. During the analysis for putative binding sites, several sites demonstrated a high score indicating possible locations of a calmodulin-binding site (Figure 25).

Figure 25. Analysis of the sequence of fesselin using the program “Calmodulin target database”. High scores indicate the possible location of a calmodulin-binding site.

```
....1 …….MGTGDYICIA   MSGGAPWGFR  LQGGKEQKQP  LQIAKVRNKS  KAAKAGLCEG
.....  0000000000 0000000000 0000000013 5555555555 5555555531

...51 DEVVSINGKP  CGDLTYAEVI  VLMESLTDVL  QMLIKRSSSG   INETFSAEKE
..... 0000000000 0000000000 0000000000 0000000000 0000000000

..101 NGKHDNIKNE  DYRESTTLQI   NTAKEIPHGD  LCITEIYSET  HQGAGESNMH
....  0000000000 0000000000 0000000000 0000000000 0000000000

..151 FSEKKQETTQ  SHRITPKVIG   TSKALVTDES  AFRGKTEERR  PSKMVELQLS
..... 0000000000 0000001111 1111111111 1111110000 0000000000

..201  LSNDGHKSTN  APAVTLIGAE  KCTPSGRGPS  VQEDGTSPVI   AIPLSVKEGN
..... 0000000000 0000000000 0000000000 0000000000 0000000000

..251 IQWSSKVVQF  SSSKEVKRIQ   SAAPSIPRVE VILACSDREK   EGPTSLAERG
..... 0000000000 0000000000 0000000000 0000000000 0000000000

..301  CVDSQVEGGQ  SEAPPSLPSF  AISSEGTEQG  EDNQHSERDH  RPLKHRARHA
..... 0000000000 0000000000 0000000000 0000000000 0000000000

..351 RLRRSESLSE  KQVKEAKSKC  KSIALLLTAA  PNPNSKGVLM   FKKRRQRARK
..... 0000000113 5799999999 9999999775 3100011355 5555555555

..401 YTLVSYGTGE LERDEDEGEE   GEVEEGDKEN   TFEVSLLATS  ESEIDEDFFS
..... 5555533100 0000000000 0000000000 0000000000 0000000000

..451 DIDNDKKIVT  FDWDSGLLEV   EKKTKSGDEM QTLPETTGKG   ALMFARRRQR
..... 0000000000 0000000000 0000000000 0000000000 0000000000

..501 MDQITAEQEE  MKARTMHAEE  QREVTVSENF  QKVSSSAYQT   KEEETLRQQP
..... 0000000000 0000000000 0000000000 0000000000 0000000000

..551 CISKSYADVS  QNDGKTVQQN  GFGLAPDTNL   SFQSSEAQKA  ASLNRTAKPF
..... 0000000000 0000000000 0000000000 0000000000 0000000000

..601 PFGVQNRAAA  PFSPTRNVTS  PLSDLPAPPP   YCSISPPPEA  LYRPLSAPAA
..... 0000000000 0000000000 0000000000 0000000000 0000000000

..651 SKAAPILWSH  TEPTERIASR  DERIAVPAKR   TGILQEAKRR  STSKPMFSFK
..... 0000000000 0000000000 0001333333 3333333333 3333333330

..701 EAPKVSPNPA  LLSLVHNAEG  KKGSGAGFES  GPEEDYLSLG   AEACNFMQSQ
..... 0000000000 0000000000 0000000000 0000000000 0000000000

..751 ASKQKAPPPI  APKPSLKVSP  AAGTPVSPVW  SPAVASNKAP   SFPAPASPQA
..... 0000000000 0000000000 0000000000 0000000000 0000000000

..801 AYPAAPKSPQ  YPHSPSANPP  NTLNLSGPFK  GPQATLASPN   HPAKTPTTPS
..... 0000000000 0000000000 0000000000 0000000000 0000000000

..851 AGETKPPFEM  PPDMRGKGAQ   LFARRHSRME KYVVDSETVQ   ANMARASSPT
..... 0000000000 0000111111 1111111111 1111000000 0000000000

..901 PSLPASWKYS  SNVRAPPPVA  YNPIHSPSYP   PAATKPFPKS  TAATKNTKRK
..... 0000000000 0000000000 0000000000 0000000000 0000000000

..951 PKKGLNALDI  MKHQPYQLDA  SLFTFQPPSN  KESLATKQIP   KLPTSKQAMS
```

```
..... 0000000000 0000000000 0000000000 0000000000 0000000000

.1001 FRLPGSGSPT  NARASSVYSV  PAYSSQPSFQ  SNASTPVNES  YTPTGYSAFS
..... 0000000000 0000000000 0000000000 0000000000 0000000000

.1051 KPESTTSSLF  TAPRPKFSAK  KAGVIAQVSG  RSLSLPGKPS   FISRATSPTS
..... 0000000000 0000000000 0000000000 0000000000 0000000000

.1101 PLIFQPAPDY  FSKPDTAADK  PGKRLTPWEA  AAKSPLGLVD   EAFGPQNMQE
..... 0000000000 0000000000 0000000000 0000000000 0000000000

.1151 SIAANVVSAA  HRKMLPEPPD   EWKKKVSYDP PGPSASLALL   GGKQPGVTAA
..... 0000000000 0000000000 0000000000 0000000000 0000000000

.1201 RKSSLSVSNA  TTQAGSQQQY  AYCSQRSQTD   PDIMSMDSRS  DYGLSTADSN
..... 0000000000 0000000000 0000000000 0000000000 0000000000

.1251 YNPQPKGWRR PT
..... 0000000000 00
```

Also during earlier experiments performed in our lab, a fragment of fesselin that bound to actin and calmodulin was generated. By MALDI-TOF fingerprint analysis, it was determined to represent the amino acids 831 to 962 of fesselin sequence from meleagris gallopavo {GenBank: ABU55374.1}.

The program PONDR predicts a short dip below the threshold of 0.6 with the extensive flanking disordered regions in the area of amino acids 865-884 corresponding to a predicted calmodulin-binding site (Figure 26). This correlates perfectly with the generalizations established for α-MoREs (Oldfield et al. 2005), short regions that undergo coupled binding and folding within a longer region of disorder.

We chose to clone and express a fragment containing amino acids 865 to 884 (Figure 27). This predicted Ca^{2+}-calmodulin binding site scored low according to the program “Calmodulin target database”, but the experimental evidence of binding overrode a theoretical prediction.

Figure 26 Possible location of a MoRE in the sequence of fesselin as predicted by PONDR.

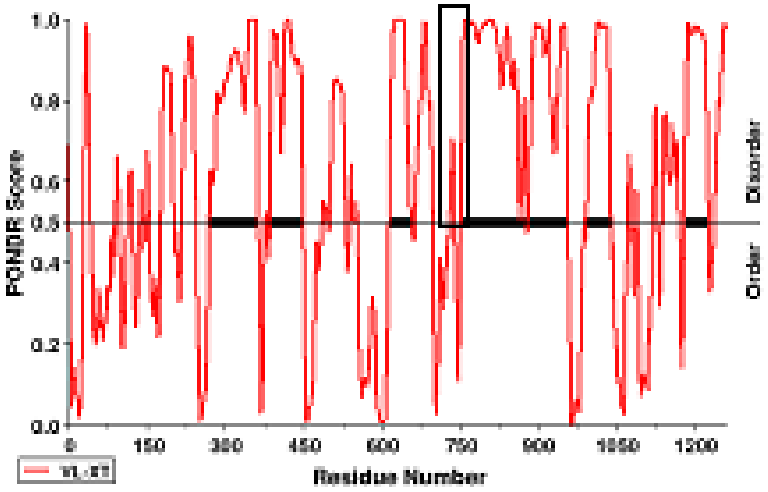
1.0
0.8
0.6
0.5
0.4
0.2
0.0
PONDR Score
Disorder
Order
0
150
300
450
600
750
900
1050
1200
Residue Number

Figure 27 Diagram showing the amino acid sequence for the fesselin 10 kD fragment

MRGKGAQ LFARRHSRME KYVVDSETVQ ANMARASSPT PSLPASWKYS SNVRAPPPVA YNPIHSPSYP PAATKPFPKS TAATKNTKRK PKKGLNALDI

Results

No expression of the fesselin 10kD fragment subcloned into pSBETA vector in E.coli

cDNA sequence of 10 kD fesselin fragment was subcloned into pSBET-A vector and overexpressed in E.coli. The cells were allowed to grow for different times varying form 1 hour to 20 hours. The fragment could not be expressed to a detectable amount (Figure 28). Other conditions tested include: LB or YTA expression medium with or without 2% glucose; expression temperature 37^0C or 20^0C; concentration of IPTG used to induce expression 0.1-0.4 mM.

No expression of a Glutathione-S-Transferase (GST)-fused or an intein-fused 10kD fragment of fesselin in E.coli

The cDNA sequence corresponding to the 10 kD fesselin fragment was subcloned into pGEX-3X vector and into pTYB1 vector and overexpressed in E.coli both as a GST-fusion and an intein-fusion protein, respectively. The cultures were grown at various temperatures until their absorbance at 600 nm reached 0.6. At this point expression of fesselin fragment was induced by adding different concentrations of IPTG. The cells were allowed to grow for different times and harvested. The fragment could not be detected in either case (Figure 29). Conditions tested include: LB or YTA expression medium with or without 2% glucose; growth temperatures 37^0C, 20^0C or 10^0C; concentration of IPTG used to induce expression 0.1-0.4 mM; incubation time after induction 1 hour to 20 hours.

Figure 28. SDS-gel showing no overexpression of 10kD fesselin fragment in E.coli. Lane A – molecular weight standards. Lane B – expression of an empty vector. Lanes C-F – no expression of the fesselin fragment. The arrow indicates the expected position of the 10kD fragment.

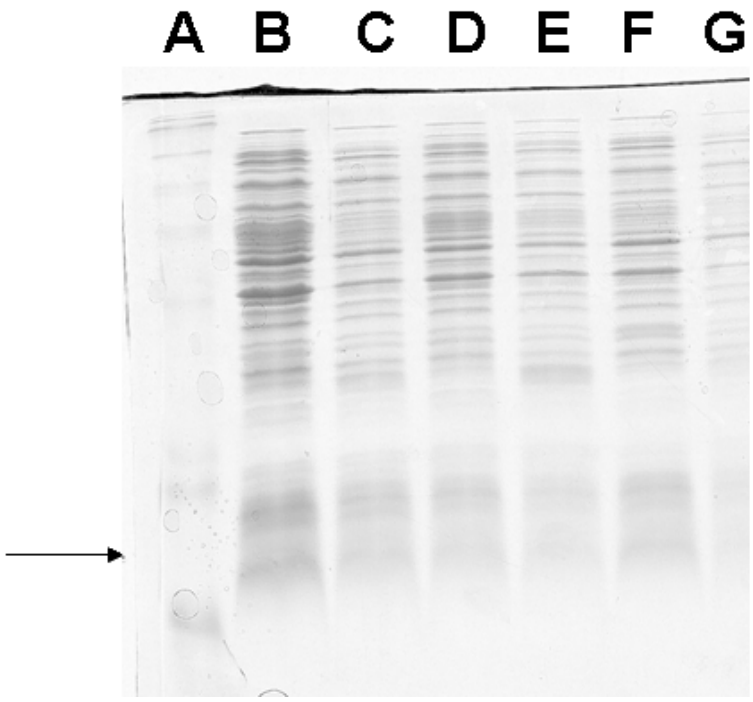
A B C D E F G

FIGURE 29. SDS-gel showing no overexpression of GST-fused 10kD fesselin fragment in E.coli Lane A – expression of GST in E.coli. Lanes B-E – no expression of GST-Fesselin fusion protein under different conditions. The oval arrow indicates the position of GST tag, the diamond arrow indicates the expected position of the fusion protein.

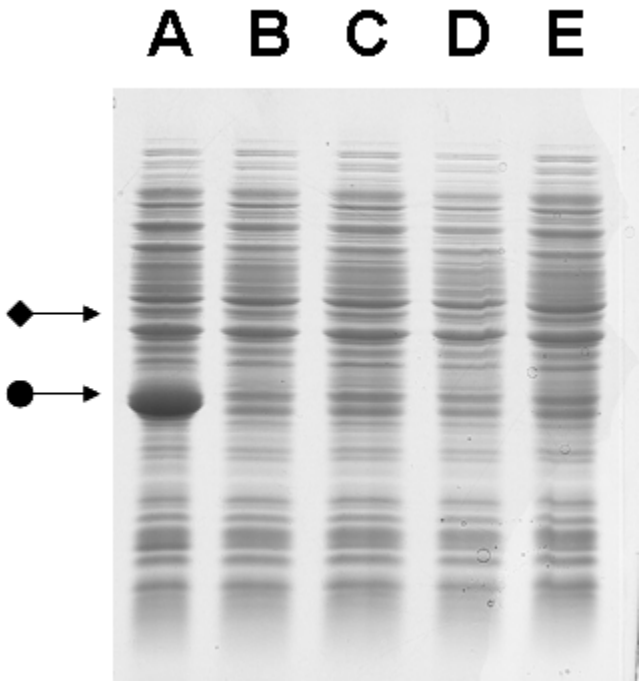
A B C D E